TECHNICAL REPORT STANDARD TITLE PAGE

1. Report No.	2. Government Accession No.	3. Recipient's Catalog No.
4. Title and Subtitle RHEOLOGICAL RESPONSE OF ASPHALTS		5. Report Date August 1972 6. Performing Organization Code
7. Author(s) David L. Allen		8. Performing Organization Report No. 333
9. Performing Organization Name and Address Division of Research Kentucky Department of Highways 533 South Limestone Lexington, Kentucky 40508		10. Work Unit No. 11 Contract or Grant No. KYHPR- 64-20
12. Sponsoring Agency Name and Address		13. Type of Report and Period Covered Final 14. Sponsoring Agency Code

15. Supplementary Notes

Prepared in cooperation with the US Department of Transportation, Federal Highway Administration

Study Title: Flexible Pavement Studies Using Viscoelastic Principles

16. Abstract

The rheological response of asphalt cements to shearing stresses is presented. The behavioral characteristics were measured using a rotating coaxial cylinder viscometer. Little or no development of theory is presented.

The viscoelastic portion of deformation is discussed in terms of the creep function. Plastic deformation is described using the definitions of apparent and plastic viscosities. Curves showing the effects of temperature, stress level and penetration on these two major components of strain are presented and discussed. Analysis indicated that plastic deformation is the predominante component of strain and, thus, should be considered and incorporated in the design of flexible pavements.

17. Key Words Apparent Viscosity, Asphalts, Creep Function, Plastic Strain, Plastic Viscosity, Viscoelastic Strain.	18. Distribution Statement

19. Security Classif. (of this report)	20. Security Classif. (of this page)	21. No. of Pages	22. Price
Unclassified	Unclassified		

Form DOT F 1700.7 (8-69)

Research Report
333

RHEOLOGICAL RESPONSE OF ASPHALTS

Final Report
KYHPR-64-20; HPR-1(8), Part II

by

David L. Allen
Research Engineer Associate

Division of Research
DEPARTMENT OF HIGHWAYS
Commonwealth of Kentucky

in cooperation with the
U. S. Department of Transportation
Federal Highway Administration

August 1972

TABLE OF CONTENTS

INTRODUCTION

Recently, considerable attention has been directed toward theoretical methods for predicting behavior of asphaltic pavements under various conditions of loading. An important factor in pavement design is the mechanical behavior of asphalt. This study is an attempt to describe that behavior. At present, most flexible pavement designs are based primarily on the elastic theory of design and(or) somewhat empirical methods. Research and experience have indicated that the reaction of an asphalt to stress is partially elastic and partially viscous; it behaves, therefore, as a viscoelastic material. Precise objectives of this study were: 1) to describe and analyze the rheological (time-dependent) behavior of asphalts and 2) to further verify results presented by Mossbarger and Deacon *(4)*.

In 1967, nineteen asphalt samples were received from the Division of Materials. Those samples had been obtained by the Division of Materials for purposes of testing and approval for various construction projects located throughout the state. The only information available on those samples was the name of the supplier, point or city from which they were shipped, and the penetration at 77° F (see Table 1). Rheological characteristics of those asphalts were determined using a concentric cylinder viscometer of the type developed by Mossbarger and Deacon *(4)*. This type of viscometer provides direct measurement of shear stress and shear rate. It consists of an inner cylinder (bob) and an outer cylinder (cup) which are mounted concentrically to form an annulus. The specimen is molded into the annulus and subjected to a shear stress by applying a torque to the bob. The angle of rotation was measured by a rotary, variable, differential transformer. A more complete description of the testing equipment, along with photographs, and description of testing procedures and method of sample preparation can be found in Mossbarger and Deacon's report *(4)*.

Three to four specimens of each sample were tested at each of three temperatures -- 39.2° F, 77° F and 104° F. Replicate specimens were subjected to a higher stress than the previous ones. Nine to twelve tests were made per sample. Durations of tests were up to 20 minutes; angle of rotation were recorded each minute throughout the test

RHEOLOGIC BEHAVIOR OF ASPHALTS

Mossbarger *(3)*, Mossbarger and Deacon *(4)*, and Saal and Labout *(5)* have described in detail the rheologic behavior of asphaltic materials. Researchers, in general, agree that asphalts behave viscoelastically within the range of temperatures employed in this study. The complex viscoelastic behavior of asphalts has often been represented by means of simple mechanical models similar to that illustrated in Figure 1(a). When stress is applied, deformation occurs; this movement is composed of three components as noted in Figure 1(b). Those components are: 1) an instantaneous, elastic deformation, represented by G_1 of Line 1, 2) a delayed, reversible component represented by G_2 and n_2 or Line 2, and 3) a plastic, irreversible component represented by n_1 and Line 3. Line 4 on Figure 1(b) is the sum of those components and represents total deformation of the rheological model. For the purposes of this study, it was assumed that there was no instantaneous, elastic deformation since no instantaneous strain could be observed experimentally. Therefore, the spring element, G_1 (Figure 1(a)), would not exist and the observed deformation would be as shown in Figures 1(c) and 1(d). In this study, flow was simply represented by the Voigt element (G_2 and n_2 in parallel), producing retarded, irreversible flow (viscoelastic), and the viscous element, n_1, producing plastic flow.

TABLE 1.

SUPPLIER, SHIPPING POINT, IDENTIFICATION AND PENETRATION OF TEST SAMPLES

SUPPLIER AND (SHIPPING POINT)	IDENTIFICATION AND PENETRATION GRADE	PENETRATION (0.1 mm, 77°F, 100 gms, 5 sec)
Ashland Oil (Ashland)	AA-5	81
Ashland Oil (Ashland)	AA-7	134
Ashland Oil (Louisville)	AL-3	52
Ashland Oil (Louisville)	AL-5	74
Ashland Oil (Louisville)	AL-7	132
Ashland Oil (Louisville)	AL-9	180
Chevron (Cincinnati)	CC-5	79
Chevron (Cincinnati).	CC-7	121
Chevron (Louisville)	CL-5	84
Chevron (Louisville)	CL-7	128
Chevron (Louisville)	CL-9	201
Ky Asphalt Sales (Kuttawa)	KK-5	86
Ky Asphalt Sales (Kuttawa)	KK-7	125
Ky Asphalt Sales (Louisville)	KL-3	56
Ky Asphalt Sales (Louisville,	KL-5	85
Ky Asphalt Sales (Louisville)	KL-7	111
Sinclair (Louisville)	SL-3	53
Sinclair (Louisville)	SL-5	80
Sinclair (Louisville)	SL-7	122

VISCOELASTIC DEFORMATION (Creep Function)

If the strain in the dashpot, n_1, in Figure 1(c) were subtracted from the total strain of the model, the result would be a continuously increasing function with a continuously decreasing slope, eventually arriving at a constant value with the slope equal to zero (Line 1 in Figure 1(d)). The shape of the curve is determined by the ratio of G_2 to n_2 -- a ratio which is continuously decreasing with time. This curve defines the creep function.

Using the rotating, coaxial cylinder viscometer, the creep function, ψ, can be determined as

$$\psi = [\theta(t) - \Omega t]/CT \quad (\text{deg/dyne/cm}^2), \qquad (1)$$

where
- $\theta(t)$ = angle of rotation (degrees),
- T = constant torque applied to bob (dyne-cm),
- C = machine constant = $(1/4\ \pi\ L)\ (1/a_1^2 - 1/a_2^2)\ (\text{cm}^{-3})$,
- L = height of annular specimen (cm),
- t = time,
- a_1 = radius of rotating bob (cm),
- a_2 = radius of stationary cup (cm), and
- Ω = steady-state angular velocity of bob relative to cup (degrees).

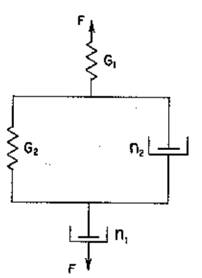

(a) SIMPLE MODEL ILLUSTRATING RHEOLOGICAL BEHAVIOR OF ASPHALTS

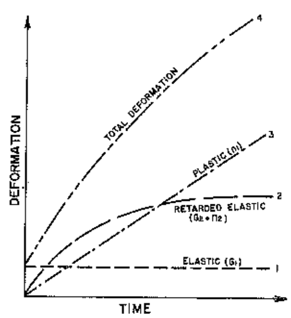

(b) CREEP CURVE FOR FIGURE 1(a)

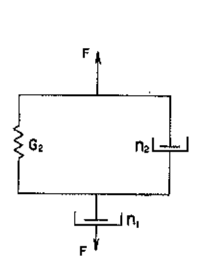

(c) SIMPLE MODEL REPRESENTING OBSERVED RHEOLOGICAL BEHAVIOR OF ASPHALTS

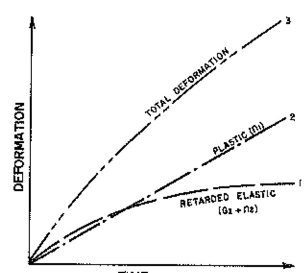

(d) CREEP CURVE FOR FIGURE 1(c)

Knowing all the constants involved and subtracting Ωt (plastic component of strain) from the total deformation, the viscoelastic strain or creep for each time interval may be calculated using Equation 1. A detailed discussion, derivations of Equation 1, and determination of constants involved may be found in Reference 4. Calculated creep functions were reduced to a standard reference temperature (509° R or 50° F) by multiplying the creep function, ψ, by the ratio of the absolute value of the test temperature to the standard reference temperature. The reference temperature was arbitrarily chosen for convenience. An example of the data is shown in Table 2.

If the viscoelastic behavior of the asphalt were linear and there were no experimental errors, tests made on one sample of asphalt and at a given temperature, but at various levels of applied shearing stress, should yield identical creep functions. However, this was not the case. There appeared to be no consistent relationship between creep function and stress level. It was suspected that inconsistencies were largely due to experimental and graphical errors. A more detailed discussion of this may also be found in Reference 4. As a result of these inconsistencies, an average creep function was calculated for each asphalt at each temperature. Those average functions have been used in the analysis throughout this report. An example of those data is also shown in Table 2 and is represented graphically in Figure 2.

The viscoelastic behavior of asphalts is dependent upon temperature and time. In order to simplify isolation of these two variables and allow the viscoelastic properties to be presented in terms of a single function, the method of reduced variables (time-temperature superposition) has been employed *(2, 4)*. In this method, the creep curve of an asphalt, determined experimentally at temperature ϕ, can be "reduced" to its position at some temperature ϕ_o by "shifting" the curve along the time axis by some predetermined amount, a_t. Thus, a series of experimental curves taken at several different temperatures, when each is reduced to ϕ_o using the appropriate value of a_t, will superpose to give a single composite curve representing the creep function at ϕ_o *(2)*.

Figure 1. Simplified Mechanical Models Representing Behavior of Asphalts.

TABLE 2.

EXAMPLE OF DATA (SAMPLE OF AL-3)

TIME (SEC)	TEMPERATURE = 39.2 °F						REDUCED AVERAGE ψ (DEG/DYNE/CM^2 x 10^4)
	LOAD						
	11,252 GMS		12,000 GMS		12,900 GMS		
	ROTATION (DEG)	ψ(DEG/DYNE/CM^2 x 10^4)	ROTATION (DEG)	ψ(DEG/DYNE/CM^2 x 10^4)	ROTATION (DEG)	ψ(DEG/DYNE/CM^2 x 10^4)	
60	4	.1773	4	.1662	4	.1546	.3333
120	6	.2660	6	.2493	5.2	.2009	.2387
180	7.4	.3289	8	.3324	6.7	.2589	.3064
240	8.9	.3945	10	.4154	9.5	.3671	.3923
300	10	.4433	11.5	.4778	11.4	.4405	.4539
360	11.2	.4965	13	.5401	13	.5023	.5130
420	12.5	.5541	14.7	.6107	14.6	.5641	.5763
480	13.7	.6073	16	.6647	16	.6182	.6301
540	15	.6649	17.7	.7354	17.2	.6646	.6883
600	16	.7092	19	.7894	18.3	.7071	.7352
660	17	.7535	20.3	.8434	19.5	.7535	.7835
720	18	.7978	21.6	.8974	20.5	.7921	.8921
780	19	.8421	23	.9555	21.5	.8308	.8761
840	20	.8865	24	.9971	22.5	.8578	.9138

TIME (SEC)	TEMPERATURE = 77 °F						REDUCED AVERAGE ψ (DEG/DYNE/CM^2 x 10^4)
	LOAD						
	200 GMS		300 GMS		4800 GMS		
	ROTATION (DEG)	ψ(DEG/DYNE/CM^2 x 10^4)	ROTATION (DEG)	ψ(DEG/DYNE/CM^2 x 10^3)	ROTATION (DEG)	ψ(DEG/DYNE/CM^2 x 10^4)	
60	5.3	.1321	8	1.3289	5	.5192	4.6468
120	10	.2492	16	2.6578	12.7	1.3188	9.3820
180	15	.3738	26.3	4.3688	20	2.0768	15.3795
240	19.8	.4934	32.7	5.4319	27	2.8037	19.2054

TIME (SEC)	TEMPERATURE = 104 °F						REDUCED AVERAGE ψ (DEG/DYNE/CM^2 x 10)
	LOAD						
	10 GMS		10 GMS		14 GMS		
	ROTATION (DEG)	ψ(DEG/DYNE/CM^2 x 10)	ROTATION (DEG)	ψ(DEG/DYNE/CM^2 x 10)	ROTATION (DEG)	ψ(DEG/DYNE/CM^2 x 10)	
60	6	.3133	9	.4700	7.4	.2747	.4571
120	11.5	.6005	16	.8355	14	.5196	.6519
180	16.2	.8459	21.4	1.1175	20.1	.7461	.9032
240	21	1.0966	26.2	1.3681	25.8	.9577	1.1408

Figure 2 shows the shift factors, a_t, for temperatures 77° F and 104° F (Sample AL-3). These factors were found graphically by shifting the curves until they coincided with the creep curve at 39.2° F. Application of the shift factors allows one to construct a composite, reduced, average, creep curve which is a function of time alone. To determine the effect of temperature on the magnitude of a_t, the log of a_t was plotted against temperature (Figure 3). The log of a_t at 39.2° F was arbitrarily plotted as zero. The curve was then adjusted until it intersected the reference temperature of 50° F (at log a_t = 0). Shift factors for 50° F were then computed as shown in Figure 3. This function describes the viscoelastic properties of asphalt in terms of temperature alone.

The shift factors, as calculated in Figure 3, were applied to the reduced, average creep curves in Figure 2 by dividing the time at which each point occurred on one of the temperature curves by its respective a_t, calculated at that temperature. A plot of these reduced, average creep functions, $\psi(\phi/\phi_o)$, against this reduced time quotient, t/a_t, resulted in a "master" creep curve which is a function of both temperature and time.

The master creep curves are significant and describe the viscoelastic behavior of an asphalt, at some specific temperature, over a range of time which normally could not be accomplished experimentally. Therefore, by performing a series of tests at a number of different temperatures over a very limited time range, one may effectively describe the behavior of a material over a much longer time span by the method of reduced variables (time-temperature superposition). The master creep curve of Asphalt AL-3 is shown in Figure 4; the remainder of the master creep curves are included in the APPENDIX.

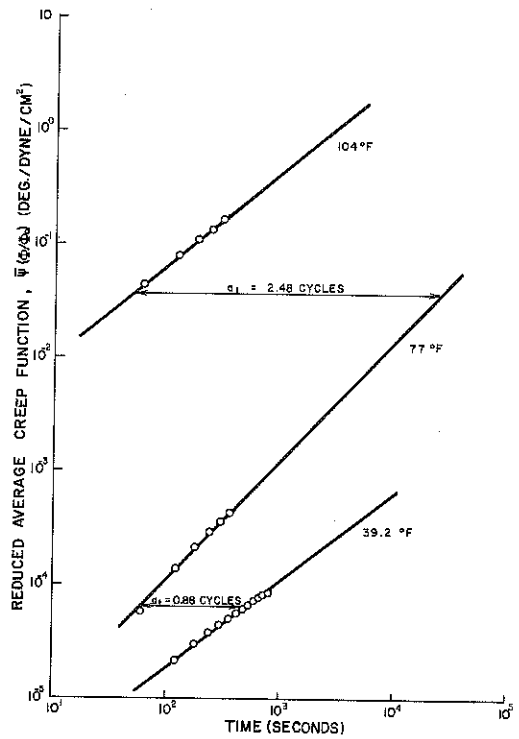

Figure 2. **Reduced Average Creep Function for Asphalt AL-3.**

If the value of the creep function, $\psi(\phi/\phi_o)$ (taken at reduced time t/a_t equal to 10^4 seconds/second) is plotted against penetration (0.1 mm, 100 grams, 77° F, 5 seconds), Figure 5 results. This plot lends support to the idea that as penetration increases the shearing resistance of the sample decreases. Two notable exceptions were the KK and AA samples. An investigation of the data on those two samples gave no indication that large experimental errors were involved.

Figure 6 is a plot of the logarithmic slope of each of the master creep curves versus penetration grade. All samples, except those from Ashland Oil, showed an increase in the magnitude of the logarithmic slope for each increase in penetration grade. Figure 5 indicated that, in general, shearing resistance of asphalts decreases as penetration increases; however, Figure 6 shows that, for samples exhibiting positive slopes, the viscous forces decrease more rapidly than the forces of elasticity. In the case of Sample AL, shearing resistance also decreased with increasing penetration; however, forces of elasticity decreased more rapidly than viscous forces.

In the cases of Samples AA and KK the shearing resistance apparently increased with an increase in penetration. However, Figure 6 shows that the slopes of the curves for those two samples have opposite signs. This would indicate that the ratio of viscous forces to elastic forces for penetration grade 7 is greater than this same ratio for penetration grade 5 (Sample KK). However, in Sample AA, the opposite would be true; the ratio of viscous forces to elastic forces would be smaller for penetration grade 7 than for penetration grade 5.

If the reduced average creep functions of Figure 2 were plotted arithmetically (after subtracting plastic strain), it would become immediately evident that an increase in temperature produces a corresponding decrease in the slope of the creep function when the creep functions taken at two different temperatures are compared at the same point in time. This phenomenon

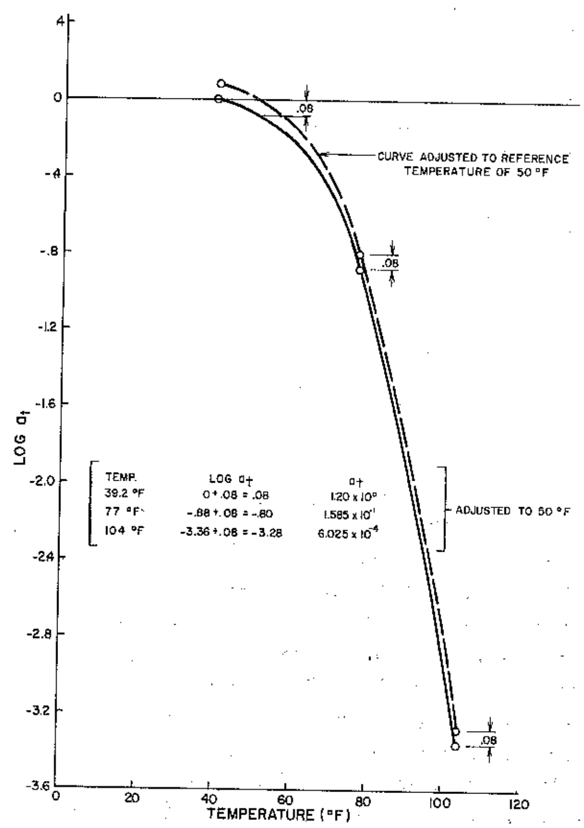

Figure 3. **Shift Factor, a_t, as a Function of Temperature.**

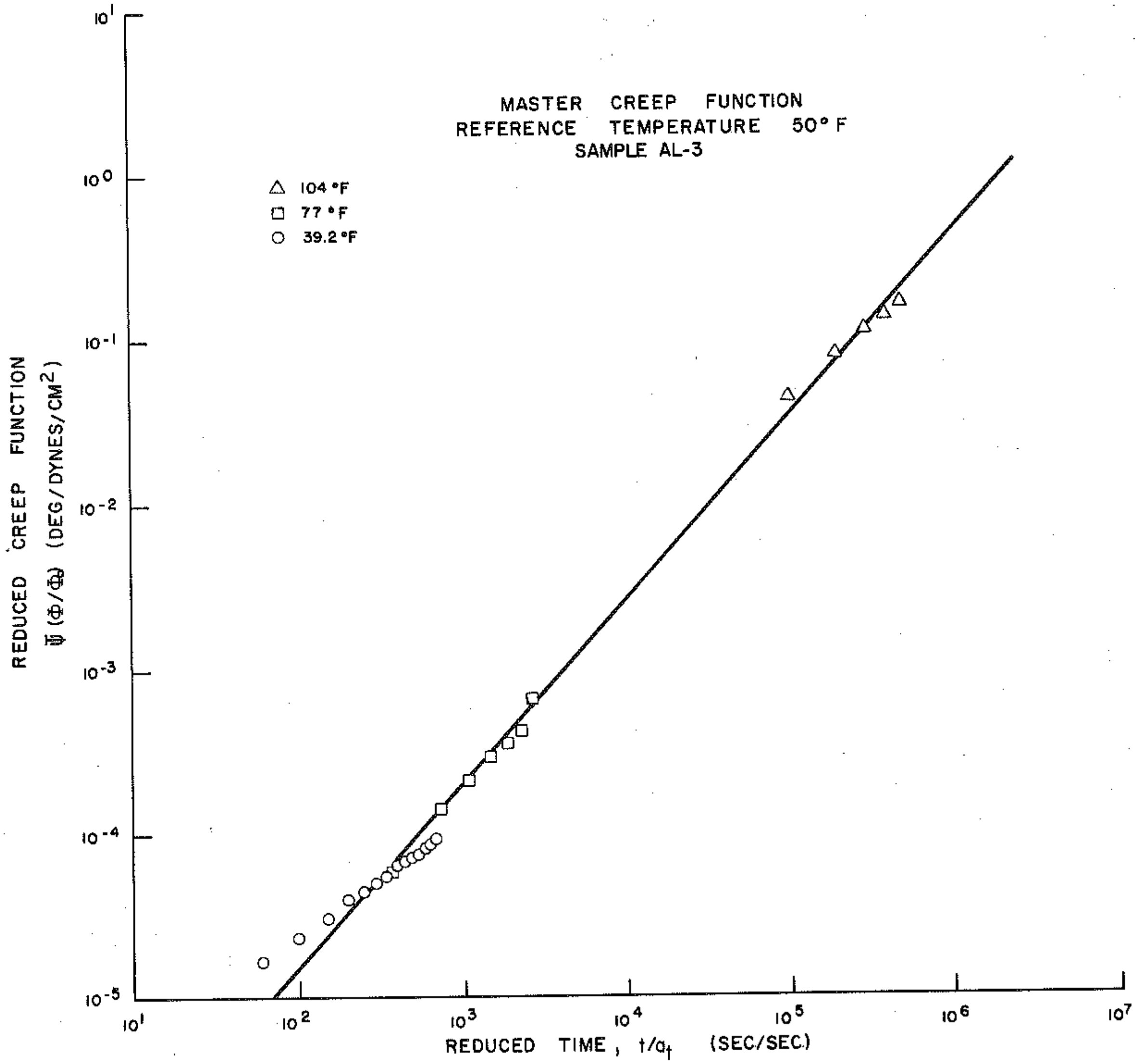

Figure 4. Master Creep Curve for Asphalt AL-3.

is a result of decreasing viscosity within the dashpot, n_2, of Figure 1(c) as the temperature increases. Consequently, the retardation times, n_2/G_2, are smaller and cause the viscoelastic portion of strain to have less effect at higher temperatures.

Data from this study would indicate that stress level does not affect viscoelastic strain; whereas, an increase in temperature causes the viscoelastic component of strain to decrease with a corresponding increase in plasticity.

PLASTIC DEFORMATION

The plastic, irreversible deformation of an asphalt is contributed by the dashpot in Figure 1(c) and is represented by Line 2 in Figure 1(d). The plastic component of strain can easily be evaluated by calculating the slope of the total deformation curve (Line 3 in Figure 1(d)) in the steady-state or linear portion of the curve. It is from this plastic component or steady-state flow that values for apparent and plastic viscosities are derived.

Apparent Viscosity

Apparent viscosity may be defined as the ratio of shearing stress to rate of shear and, for non-Newtonian liquids, is dependent upon rate of shear and, in some instances, upon shearing stress. Using the rotating coaxial cylinder, apparent viscosity is computed as follows:

$$n_a = CT/\Omega \qquad (2)$$

where n_a = apparent viscosity. In order to compute the angular velocity, a plot of angle of rotation against time was made, as shown in Figure 7. Angular velocity may then be defined as the quotient of angle of rotation and elapsed time. Therefore, from Figure 7 it becomes obvious that angular velocities for times t_1 and t_2 are θ_1/t_1 and θ_2/t_2, respectively. However, Ω_1 is greater than Ω_2. Under these experimental conditions, apparent viscosity is obviously a function of shear rate and shearing stress *(4)*. Because of dependence on these two factors, angular velocity is redefined in Equation 2 as the velocity in the region of steady-state flow. Figure 7 shows that is the region where a linear relationship exists between angle of rotation and time. Thus, the steady-state angular velocity in Figure 7 is defined as $\Delta\theta/\Delta t$. In this study, all apparent viscosities were calculated using Equation 2 and the aforementioned definition of angular velocity. A more thorough and complete discussion of apparent viscosity is given in Reference 4.

Rheological characteristics of asphalts are highly dependent on temperature. For example, there is a considerable decrease in viscosity as temperature increases. Figures 8 and 9 are plots of apparent viscosity versus the inverse of temperature ($°R^{-1}$) and clearly exhibit that relationship. High-temperature viscosities, $1.36 \times 10^{-3} °R^{-1}$, were found according to AASHO Standard Test T 201-65 for kinematic viscosity, and the results were converted to apparent viscosity. A careful examination of both figures reveals that samples having lower penetration values, in general, had a higher viscosity at any given temperature than did samples with higher penetration values. The notable exception to this was the PAC-3 sample (AL-3). At a temperature of 275°F ($1/\phi = 1.36 \times 10^{-3}\ °R^{-1}$), this sample had a viscosity value approaching that of the two PAC-7 samples -- a value smaller than all of the PAC-5 samples. On an arithmetic plot, these curves show a pronounced and rapid convergence (between penetration grades) toward the high temperature end; in the range of temperatures used in this study, the curves would be diverging toward the low temperatures.

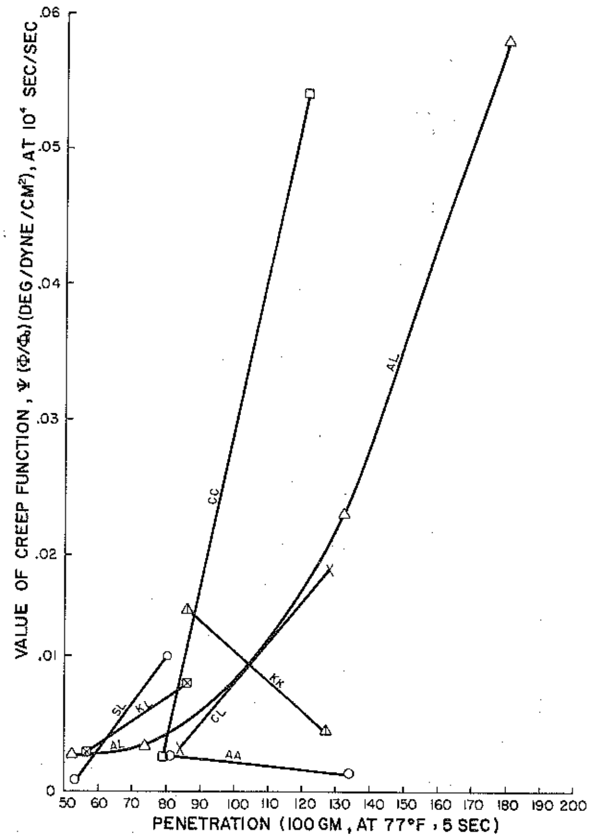

Figure 5. Effect of Penetration on Master Creep Function.

At temperatures below 39.2°F ($1/\phi = 3.0 \times 10^{-3}\ °R^{-1}$), it is suspected the curves would again converge as the temperature continued to decrease, and the "stiffness" (stiffness = 3 x viscosity/loading time) would tend to reach a maximum at approximately 2.5 - 3.0 x 10^{10} dynes/cm^2; this is often identified as the "glassy zone". This should hold true because, at low temperatures, it is predominantly elastic forces which determine the character of the deformation; therefore, the stiffness should approach the value of Young's modulus for all bitumens, causing the curves to converge *(5)*.

Figures 8 and 9 show that as temperature increases above 140°F ($1/\phi = 1.57 \times 10^{-3}\ °R^{-1}$), the slope of the curves decrease rapidly to nearly horizontal, indicating that any further increase in temperature would produce little change in the viscosity. It appears that all asphalts tested would have an approximate minimum viscosity ranging from about 150 to 400 poises. This sudden change in slope of the curve appears to occur at a point where many of the solid or semisolid bodies in the asphalt have melted. After most of the solid material liquifies, further heating produces little change in viscosity.

In the linear portion of the curves, there is a continuously changing relationship between the elastic and viscous forces in the asphalt. The ratio of elastic to viscous forces is a rapidly decreasing function, starting from a maximum at the low end of the temperature spectrum. This occurs first as a result of increased mobility of the solid particles and finally, as temperature continues to increase, the increased mobility of the long, hydrocarbon molecular chains *(1)*.

Relationships between apparent viscosity and penetration at temperatures of 39.2°F, 77°F, and 140°F are shown in Figures 10 through 12. These figures show a definite trend with the lower penetration numbers exhibiting higher viscosities. Differences in penetration had decreasingly less effect with increasing temperature. In going from 140°F to 77°F, the viscosity increased 33,470 percent. Further decrease in temperature from 77°F to 39.2°F produced an additional decrease of 35,000 percent. The variability of the viscosity of asphalts, expressed as the ranges of measurements divided by their average values, was 326, 308, and 390 percent for 39.2°F, 77°F, and 104°F, respectively.

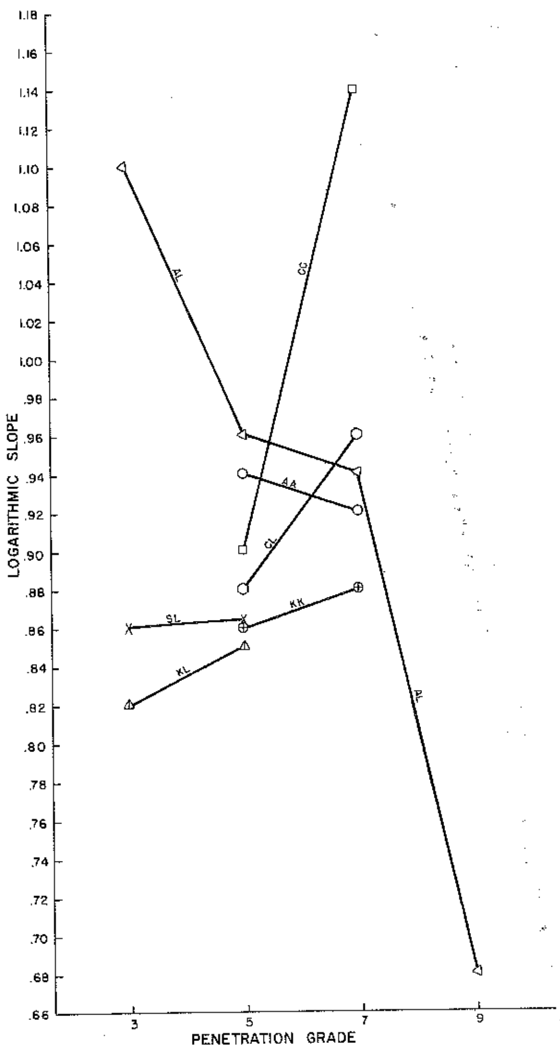

Figure 6. **Effect of Penetration on Logarithmic Slope of Master Creep Curve.**

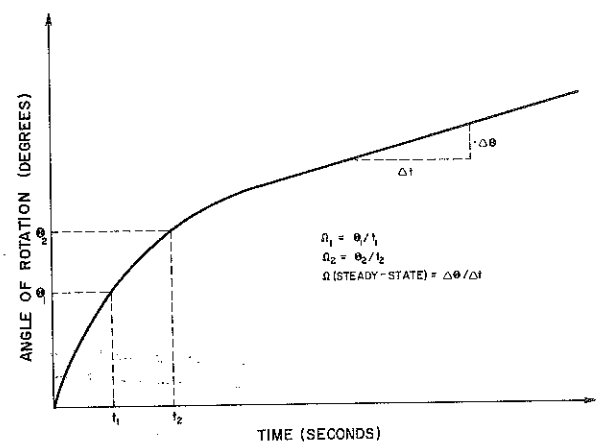

Figure 7. **Angle of Rotation as a Function of Time.**

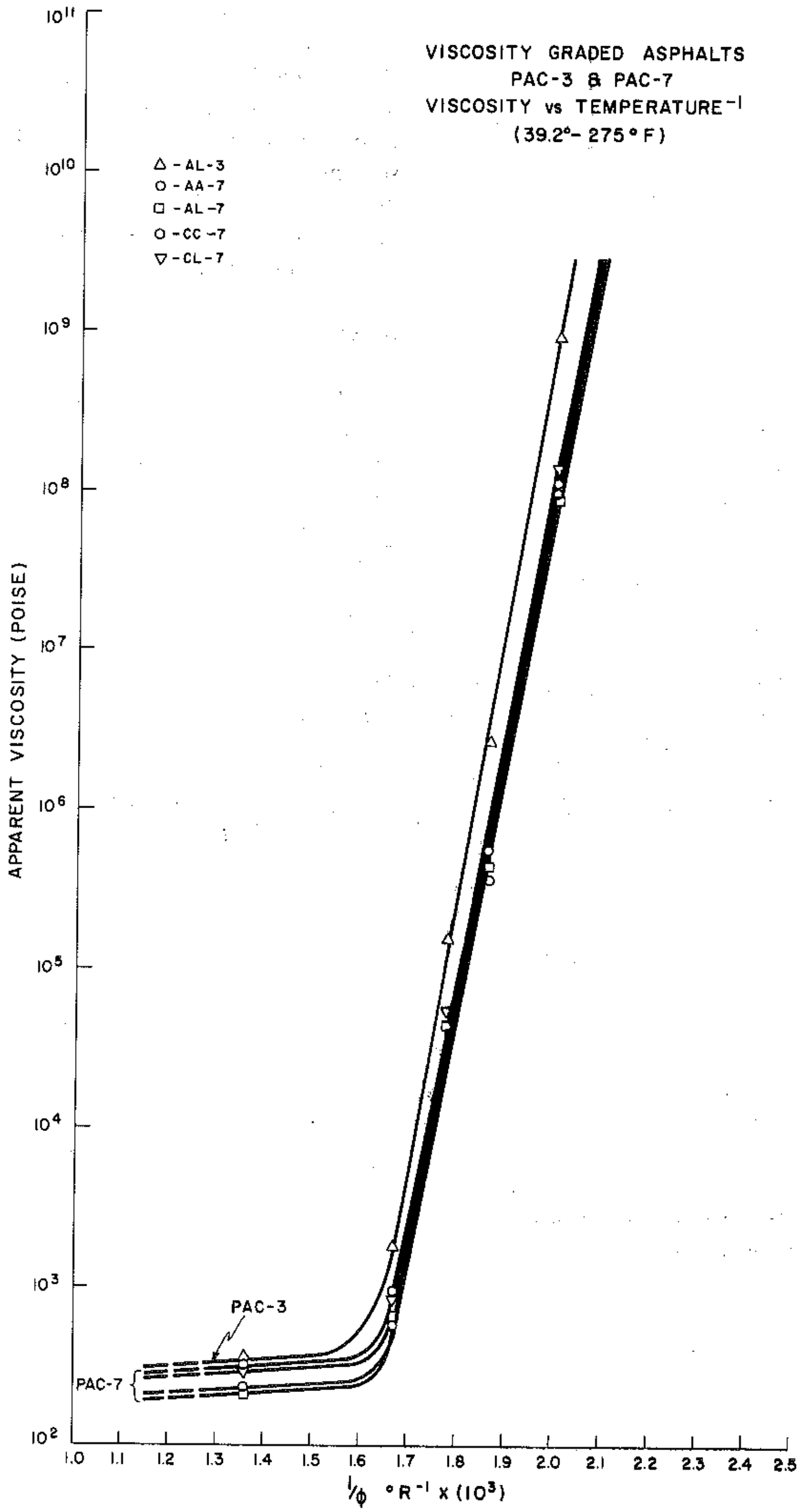

Figure 8. **Apparent Viscosity as a Function of Temperature (PAC-3 and PAC-7).**

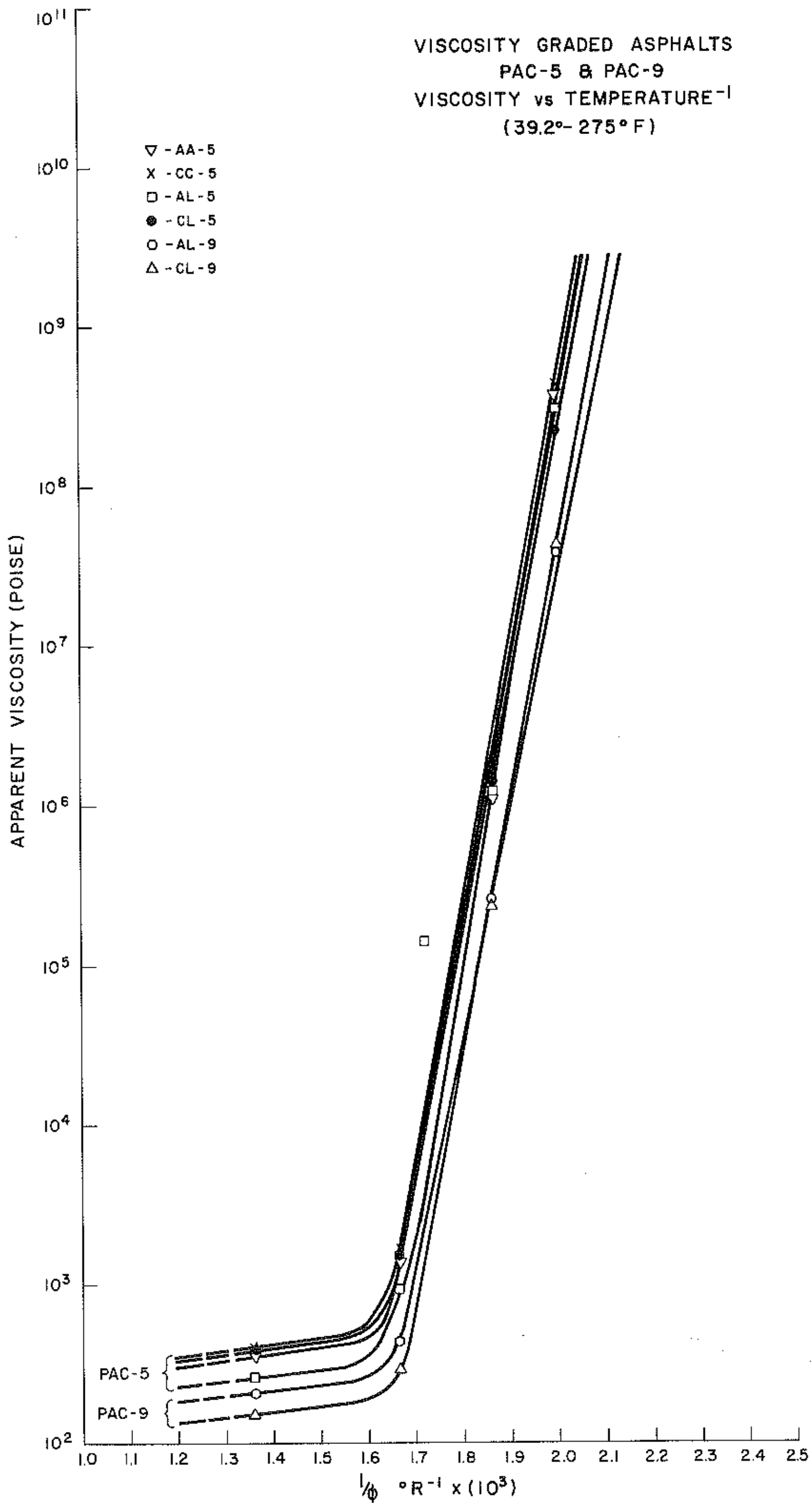

Figure 9. **Apparent Viscosity as a Function of Temperature (PAC-5 and PAC-9).**

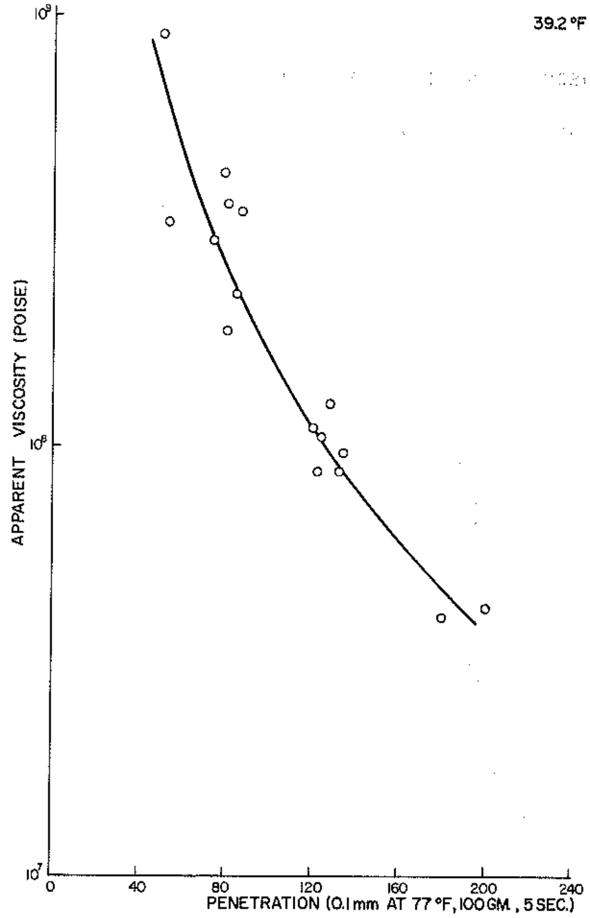

Figure 10. **Effect of Penetration on Apparent Viscosity (39.2°F).**

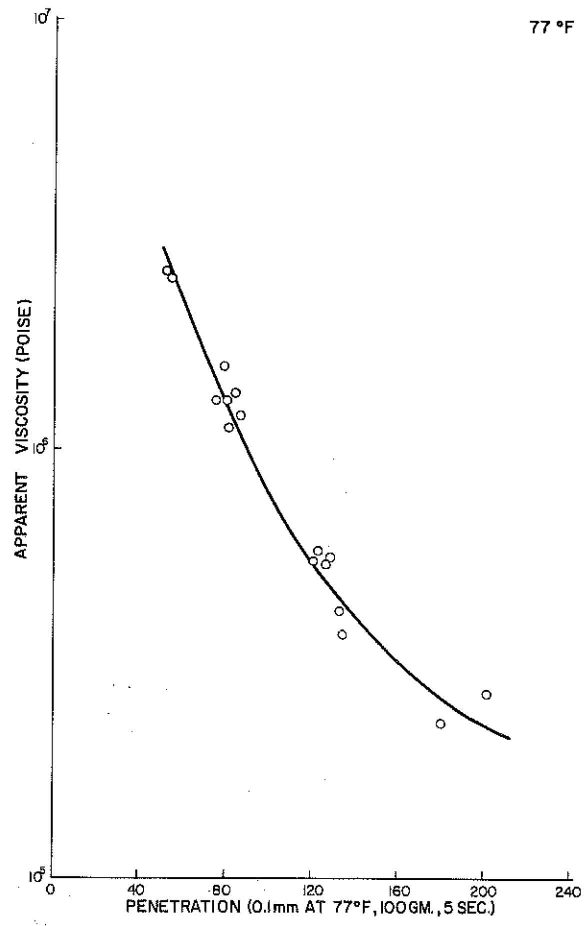

Figure 11. **Effect of Penetration on Apparent Viscosity (77°F).**

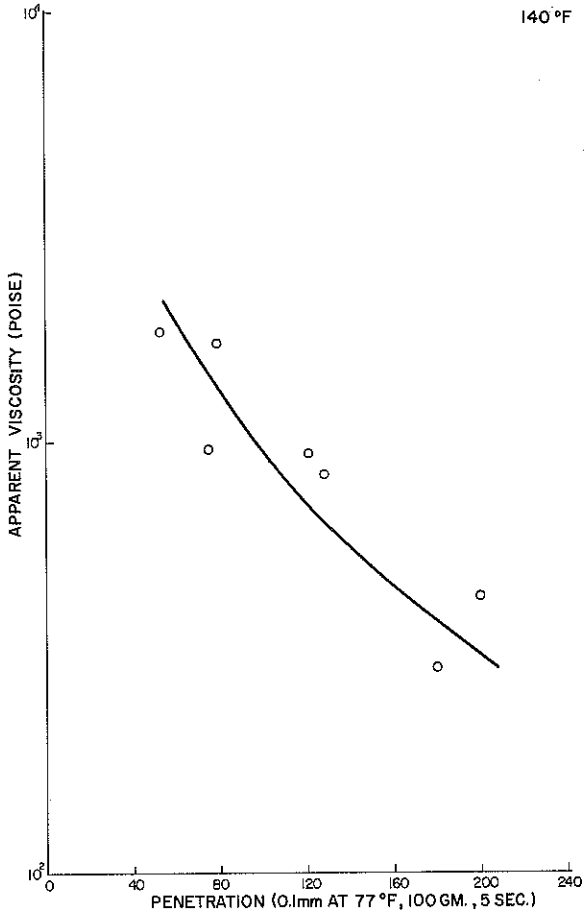

Figure 12. Effect of Penetration on Apparent Viscosity (140°F).

Plastic Viscosity

Mossbarger and Deacon *(4)* reported that the plastic viscosity measurement is a shear-independent quantity. They say, however, that "*...before evaluating the plastic viscosity, it is necessary to first establish that the behavior of asphalt cements in the steady-state flow regime may be represented by that of a Bingham plastic.*" In a rotating coaxial cylinder viscometer, a Bingham plastic would have three conditions of loading as illustrated graphically in Figure 13. The first condition is when the applied torque is less than the yield stress and no flow occurs (from 0 to T_1 in Figure 13). As the torque is increased from T_1 to T_2, partial flow occurs. This flow will occur in the material located between the surface of the bob and a critical radius, $r_c = (T/2 \Pi L S_y)^{1/2}$, where S_y is the yield stress. Further increase in the magnitude of torque beyond T_2 will produce flow throughout the material, thus creating the straight-line portion of Figure 13 *(4)*. The plastic viscosity, n_p, is then defined as the inverse of the slope of the straight-line portion. Mossbarger and Deacon *(4)* and Alfrey *(1)* have given a more thorough discussion of the behavioral characteristics of a Bingham plastic.

Figure 14 is a plot of the CT product (C = machine constant) against steady-state angular velocity, Ω, for Asphalt AL-5. This plot, along with a similar plot for each asphalt tested, indicated that asphalt cements do behave as Bingham plastics in the steady-state region. The plastic viscosity, n_p, was then computed using the definition just mentioned. Table 3 lists plastic viscosities for each asphalt at each temperature. Some of the viscosities are not listed at 39.2°F because the data, in those cases, did not show any correlation. Figures 15 and 16 are graphical representations of data listed in Table 3.

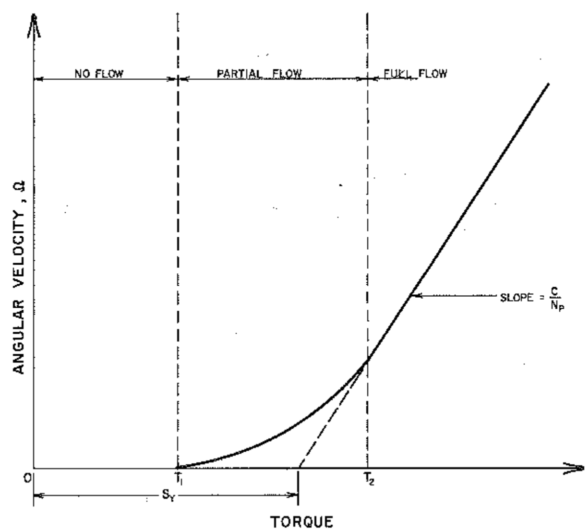

Figure 13. Angular Velocity as a Function of Torque for a Bingham Plastic.

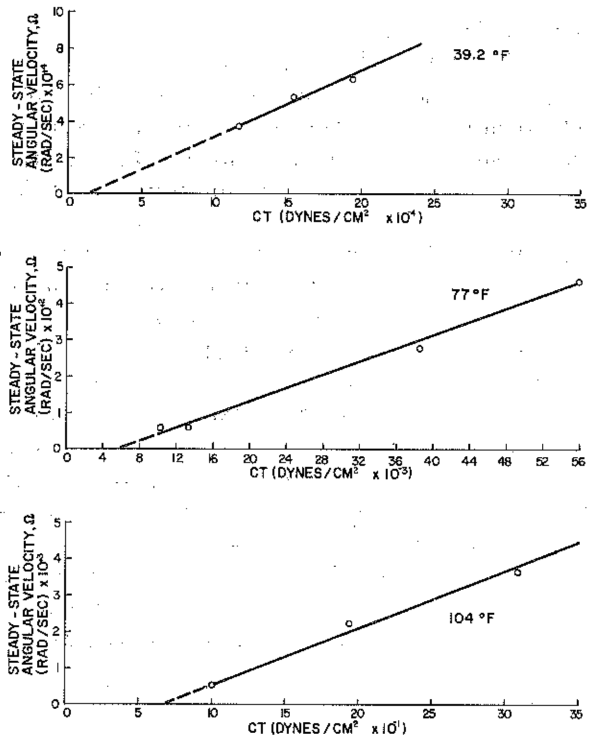

Figure 14. **Angular Velocity versus CT for Asphalt AL-5.**

One method of determining the temperature susceptibility of an asphalt is by computing the magnitude of the slope of the viscosity-temperature relationship *(4)* from

$$VTS = \frac{\log \log n_{p(1)} - \log \log n_{p(2)}}{\log \phi_2 - \log \phi_1} \tag{3}$$

where VTS = viscosity-temperature slope,
$n_{p(1)}$ = plastic velocity in poises at T_1,
$n_{p(2)}$ = plastic velocity in poises at T_2,
ϕ_1 = highest temperature in °R (104°F), and
ϕ_2 = lowest temperature in °R (39.2°F).

Because many of the plastic viscosities at 39.2°F were not available, the viscosity-temperature slope was calculated for all samples over the temperature range of 77°F to 104°F. However, in cases where the viscosity was available at 39.2°F, the viscosity-temperature slope was calculated over that range. Results are shown in Table 4.

TABLE 3.

PLASTIC VISCOSITIES

SAMPLE NO.	PLASTIC VISCOSITY @ 39.2°F (10^7 POISES)	PLASTIC VISCOSITY @ 77°F (10^5 POISES)	PLASTIC VISCOSITY @ 104°F (10^4 POISES)
AA-5	28.6	9.72	21.40
AA-7	9.1	3.27	0.95
AL-3	31.1	24.30	15.00
AL-5	27.8	11.60	6.29
AL-7		4.16	1.80
AL-9		2.01	1.41
CC-5		13.80	9.35
CC-7		4.13	4.29
CL-5	13.3	12.90	11.80
CL-7		5.55	3.39
CL-9		3.23	1.82
KK-5		11.50	8.93
KK-7		5.20	2.36
KL-3	26.0	33.20	6.02
KL-5	25.0	12.00	6.60
KL-7	14.4	7.83	5.10
SL-3		27.70	15.10
SL-5	18.3	12.60	4.44
SL-7		4.99	

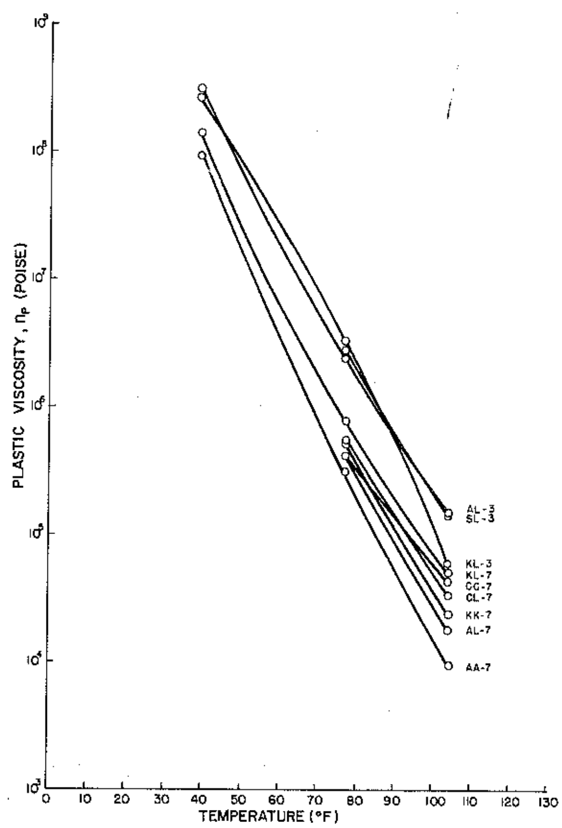

Figure 15. **Plastic Viscosity as a Function of Temperature (PAC-3 and PAC-7).**

TABLE 4.

TEMPERATURE SUSCEPTABILITY USING VISCOSITY-TEMPERATURE SLOPE

TEMPERATURE SUSCEPTABILITY (77° - 104°F)

SAMPLE	VISCOSITY-TEMPERATURE SLOPE
AA-5	2.3
AA-7	6.6
AL-3	4.2
AL-5	4.7
AL-7	5.6
AL-9	4.9
CC-5	4.3
CC-7	3.9
CL-5	3.7
CL-7	4.8
CL-9	5.2
KK-5	4.1
KK-7	5.4
KL-3	6.3
KL-5	4.7
KL-7	4.5
SL-3	4.4
SL-5	5.5

TEMPERATURE SUSCEPTABILITY (39.2° - 104°F)

SAMPLE	VISCOSITY-TEMPERATURE SLOPE
AA-5	3.7
AA-7	5.6
AL-3	4.0
AL-5	4.6
CL-5	3.8
KL-3	4.6
KL-5	4.5
KL-7	4.5
SL-5	4.7

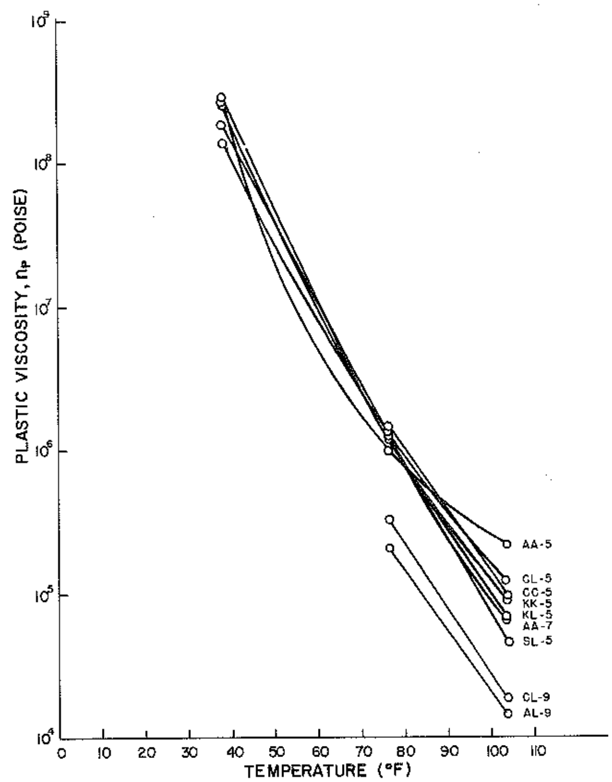

Figure 16. Plastic Viscosity as a Function of Temperature (PAC-5 and PAC-9).

There appeared to be no great difference in the temperature susceptibilities amongst the asphalt samples. There was little or no correlation in relation to sample source or to penetration grade. The most notable fact was that the sample most affected by temperature was AA-7 and the least susceptible to temperature was AA-5. Beyond stating that samples from the Ashland Oil Company and from the Ashland storage tanks had the greatest amount of variability, there are no conclusions concerning temperature susceptibility of the test samples.

Relationships between plastic viscosity and penetration are shown in Figures 17 through 19. As in the case of apparent viscosity, plastic viscosity also presented a general trend of increasing viscosity with decreasing penetration. The average viscosity increased 1,400 percent as the temperature decreased from 104°F to 77°F and increased 23,000 percent as the temperature decreased from 77°F to 392°F. Variability among the asphalts at 39.2°F, 77°F, and 104°F was 237, 315, 312 percent, respectively.

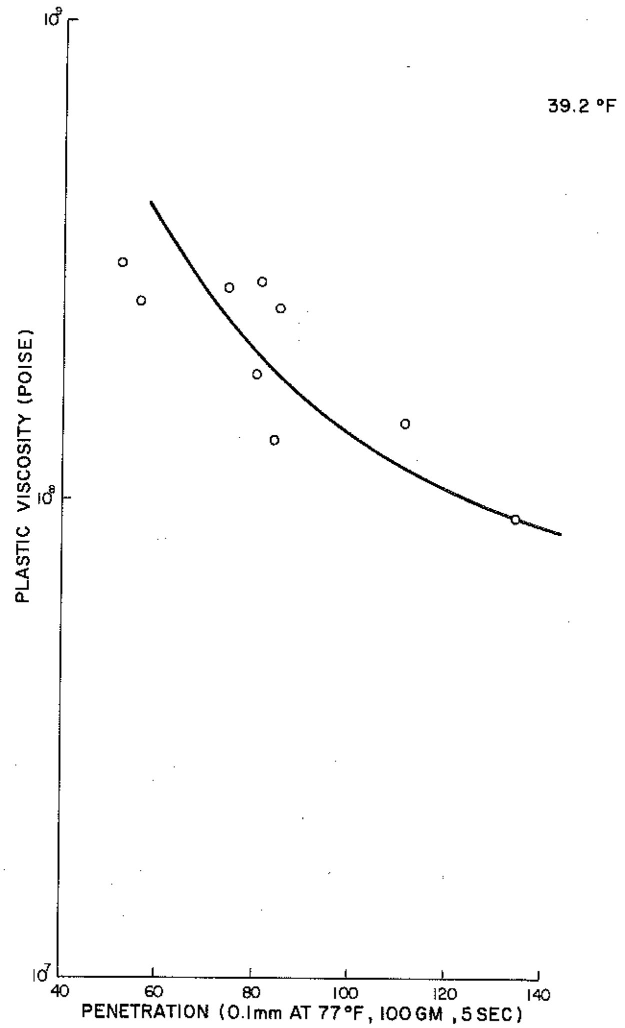

Figure 17. Effect of Penetration on Plastic Viscosity (39.2°F).

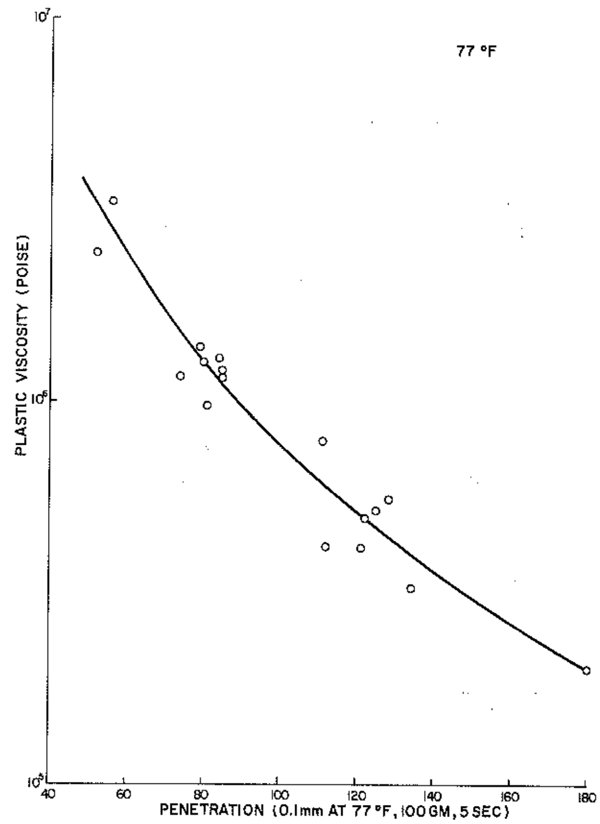

Figure 18. Effect of Penetration on Plastic Viscosity (77°F).

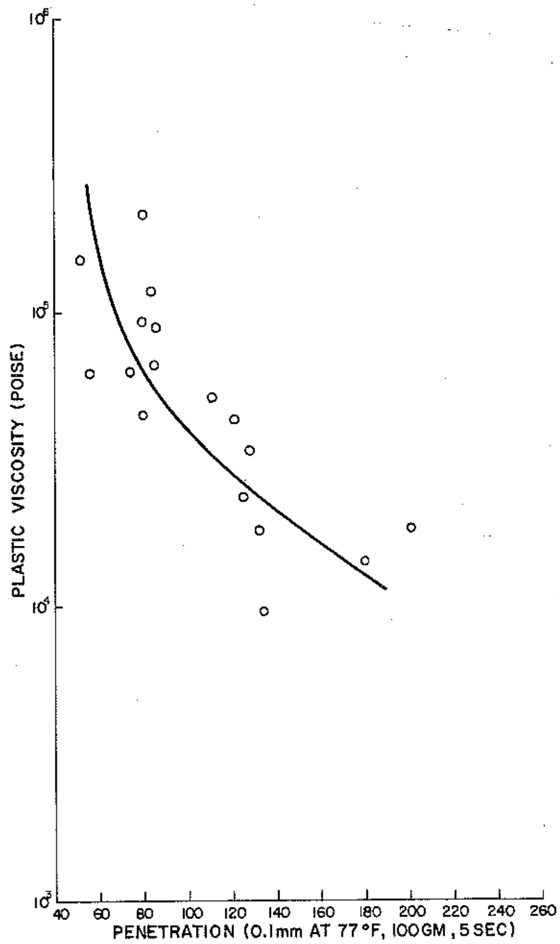

Figure 19. Effect of Penetration on Plastic Viscosity (104°F).

Apparent Viscosity-Plastic Viscosity Relationship

Mossbarger and Deacon *(4)* state that *"...the steady-state, apparent viscosities should generally exceed the plastic viscosity and should approach its value only at high shearing stresses or high rates of shear".* This statement was based upon actual data from their study In light of this statement, a graphical analysis has been made of the relationship between apparent and plastic viscosities. In Figure 20, a plot has been made of apparent viscosity versus plastic viscosity. In this analysis, the apparent viscosity was calculated using the highest shearing stress employed for that particular test specimen. This was done to determine the point at which the two viscosities were equal. Figure 20 shows, in most cases, that the approach was not successful. In cases where points fell below the one-to-one ratio line, the maximum applied shearing stress was too small for the plastic viscosity to equal the apparent viscosity; the converse would hold true for points located above the line.

Classification of Asphalts by Plastic Viscosity

In Tables 5, 6, and 7 plastic viscosity measurements have been used to classify the asphalts into viscosity intervals at the three test temperatures. These intervals were chosen so that their ranges were equal on a logarithmic plot.

Samples were generally grouped at all three temperatures, as would be expected, with the higher penetration asphalts occurring in the lower viscosity groups. In going from one temperature to another, the most notable change in grouping was Samples AA-5 and KL-3. Sample AA-5, which had the lowest temperature susceptibility, was in the highest viscosity group at 39.2°F; but at 77°F, it appeared in the fourth lowest group. Sample KL-3, having the second highest temperature susceptibility, occurred in the highest viscosity group at 39.2°F and 77°F but was in the third lowest group as it became less viscous at 104°F.

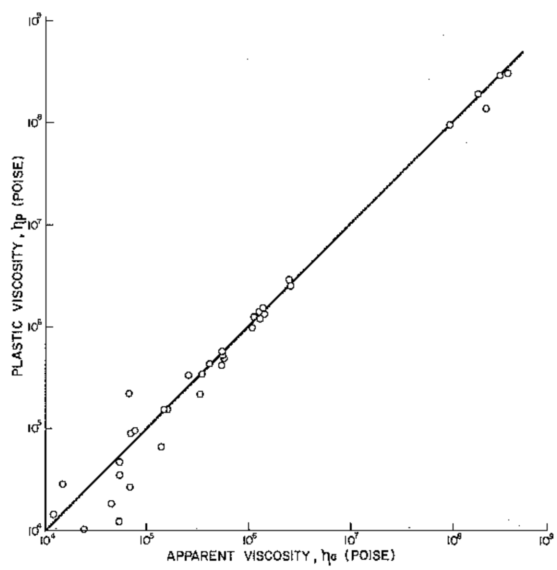

Figure 20. Apparent Viscosity-Plastic Viscosity Relationship.

TABLE 5.

CLASSIFICATION OF ASPHALTS BY PLASTIC VISCOSITY AT 39.2°F

Viscosity Interval (10^8 Poises)	Sample
0.9 — 1.4	AA-7, CL-5
1.4 — 2.3	KL-7, SL-3
2.3 — 3.6	AA-5, AL-3, AL-5, KL-3, KL-5

TABLE 6.

CLASSIFICATION OF ASPHALTS BY PLASTIC VISCOSITY AT 77°F

Viscosity Interval (10^6 Poises)	Sample
0.20 — 0.32	AL-9
0.32 — 0.51	AA-7, AL-7, CC-7, SL-7
0.51 — 0.80	CL-7, KK-7, KL-7
0.80 — 1.5	AA-5, AL-5, KK-5, KL-5
1.5 — 2.0	CC-5, CL-5, SL-5
> 2.0	AL-3, KL-3

TABLE 7.

CLASSIFICATION OF ASPHALTS BY PLASTIC VISCOSITY AT 104°F

Viscosity Interval (10^4 Poises)	Sample
0.9 — 1.8	AA-7, AL-9
1.8 — 3.6	AL-7, CL-7, CL-9, KK-7
3.6 — 7.2	AL-5, CC-7, KL-3, KL-5, KL-7, SL-5
7.2 — 14.0	CC-5, CL-5, KK-5
> 14.0	SL-3, AA-5

DISCUSSION

DATA ANALYSIS

In studying the temperature susceptibility of the asphalts, only the viscosity-temperature slope was employed. The penetration ratio was not used since only the penetration at 77°F was known. The penetration index was not computed because the ring-and-ball temperatures of the asphalts were not available.

No analysis was made involving method of refining, crude source, or asphaltene content; those factors were not determined.

Stiffness of the asphalts, a time-dependent quantity, was mentioned only in passing. Some of the specimens did not have an adequate number of readings at the beginning of the tests (less than two minutes); thus a thorough analysis could not be made.

Ferry *(2)* suggests three criteria for determining the applicability of the method of reduced variables (time-temperature superposition) to a data set: 1) exact matching of shapes of adjacent curves obtained at different test temperatures, 2) superposition of values of the shift factor for different viscoelastic functions, and 3) a reasonable form of the temperature dependence of the shift factor consistent with experience. Figure 4 and those exhibited in the APPENDIX lend support to the first criterion. The creep function was the only viscoelastic function studied; therefore, an evaluation of the second criterion cannot be made. The form of the temperature dependence of the shift factor appeared to be consistent with data obtained by other researchers *(2, 4, 5)* and seems to satisfy the third condition. It appears the method of reduced variables was a valid means of analysis for the asphalts tested and in the range of temperatures used -- assuming, of course, that the second criterion also holds true.

IMPLICATIONS OF DATA

In relation to flexible pavements, it would appear the plastic component of strain is the most critical portion. This idea is reinforced since the plastic component is the only irreversible component and, therefore, the only portion producing permanent deformation in a pavement. At higher temperatures, the largest portion of strain produced is plastic strain; as a matter of fact, at temperatures often encountered at the surface of an asphalt pavement on warm days, practically all of the deformation encountered will be plastic. This would imply, therefore, that flexible pavement design should, in some manner, incorporate plastic strain with less emphasis being placed on viscoelastic strain.

The data indicate that in trying to minimize the variability of the stress-strain properties of the asphalt over the range of temperatures encountered in the field, an asphalt with a lower temperature susceptibility would be desirable. However, the data also indicate that, at temperatures of 140°F and above, the viscosity and, consequently, the plastic properties of all asphalts appeared to be similar.

With all factors such as stress, penetration and temperature being equal, viscosity appears to give a qualitative but by no means quantitative indication of behavior; i.e., the higher the viscosity the less the plastic behavior. Likewise, a lower penetration appears to imply less plastic flow, assuming stresses and temperatures are equal. Therefore, viscosity and penetration classifications would appear to be useful in making an approximation of behavior.

REFERENCES

1. Alfrey, T., Jr., **Mechanical Behavior of High Polymers**, Interscience Publishers, Inc., New York, 1948.

2. Ferry, J. D., **Viscoelastic Properties of Polymers**, John Wiley and Sons, Inc., New York, 1961.

3. Mossbarger, W. A., Jr., *A Rheological Investigation of Asphaltic Materials,* Division of Research, Kentucky Department of Highways, January 1964.

4. Mossbarger, W. A., Jr. and Deacon, J. A., *Flow Behavior of Asphalt Cements,* Division of Research, Kentucky Department of Highways, May 1967.

5. Saal, R. N. J. and Labout, J. W. A., *Rheological Properties of Asphalts,* **Rheology, Theory and Applications**, Volume 2, F. R. Eirich, Editor, Academic Press, Inc., New York, 1956.

APPENDIX

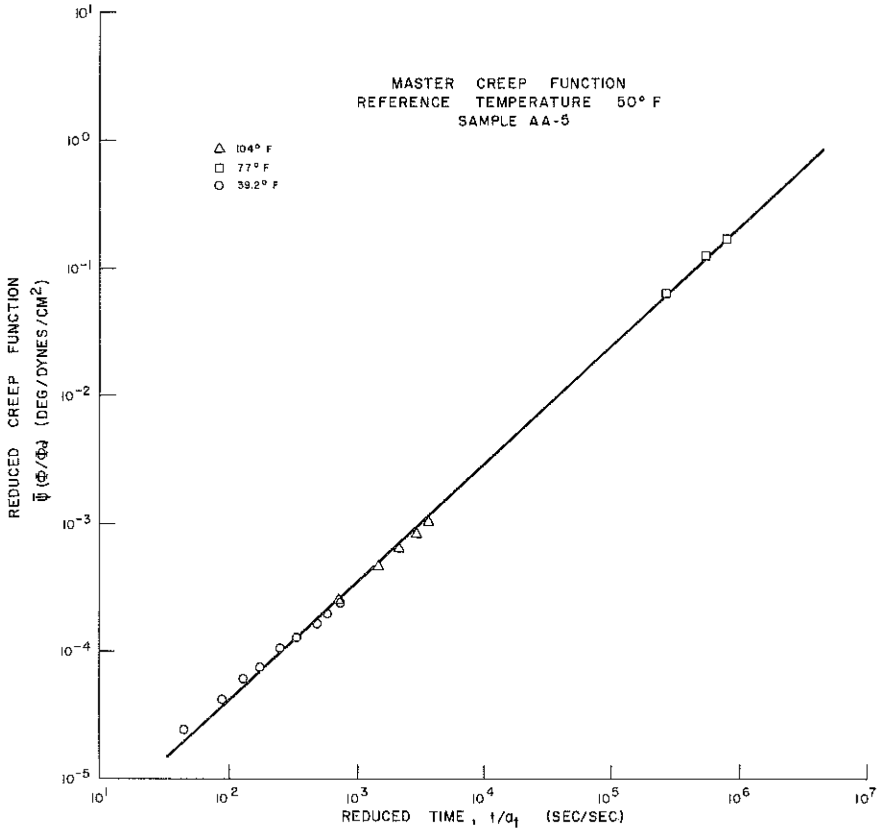
MASTER CREEP FUNCTION
REFERENCE TEMPERATURE 50° F
SAMPLE AA-5
△ 104° F
□ 77° F
○ 39.2° F
REDUCED CREEP FUNCTION
$\bar{\psi}(\Phi/\Phi_d)$ (DEG/DYNES/CM^2)
REDUCED TIME, t/a_t (SEC/SEC)
10^1
10^0
10^{-1}
10^{-2}
10^{-3}
10^{-4}
10^{-5}
10^1
10^2
10^3
10^4
10^5
10^6
10^7

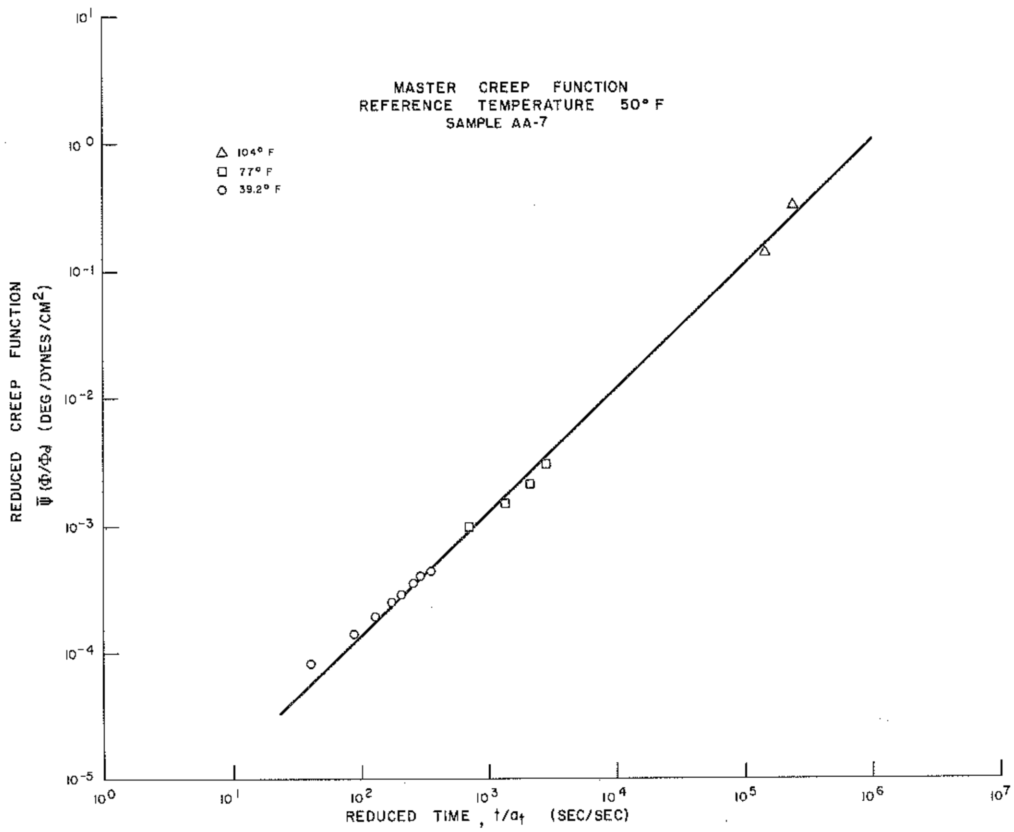
MASTER CREEP FUNCTION
REFERENCE TEMPERATURE 50° F
SAMPLE AA-7
△ 104° F
□ 77° F
○ 39.2° F
REDUCED CREEP FUNCTION
$\bar{\psi}(\Phi/\Phi_d)$ (DEG/DYNES/CM^2)
REDUCED TIME, t/a_t (SEC/SEC)
10^1
10^0
10^{-1}
10^{-2}
10^{-3}
10^{-4}
10^{-5}
10^0
10^1
10^2
10^3
10^4
10^5
10^6
10^7

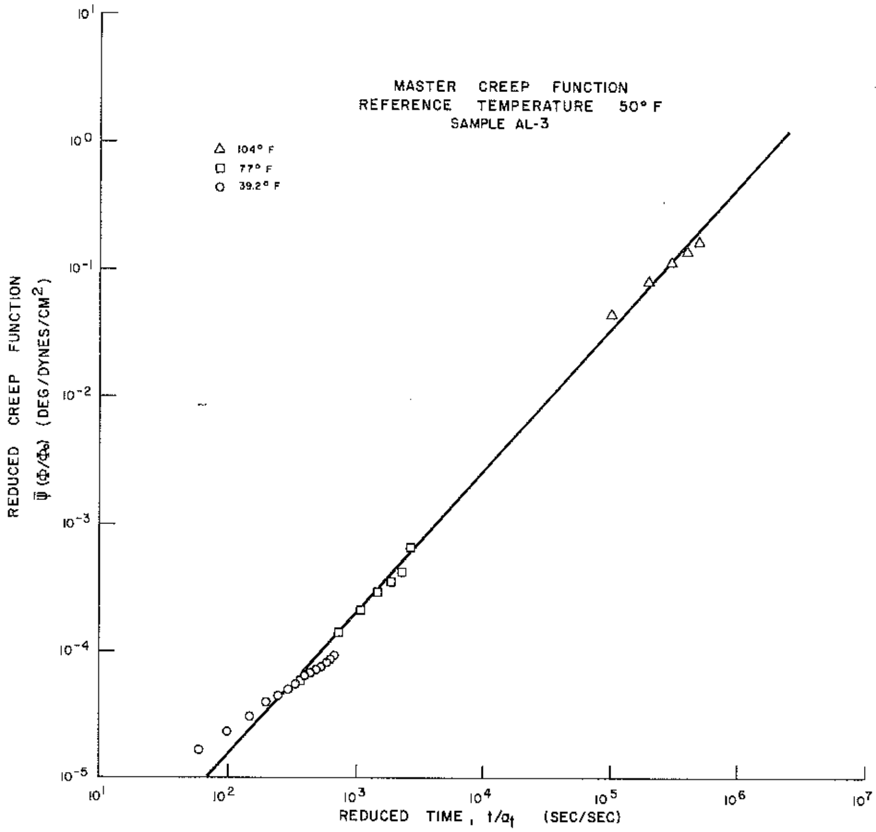
MASTER CREEP FUNCTION
REFERENCE TEMPERATURE 50° F
SAMPLE AL-3
104° F
77° F
39.2° F
REDUCED CREEP FUNCTION
$\bar{\psi}$ (Φ/Φ_0) (DEG/DYNES/CM²)
REDUCED TIME, t/a_T (SEC/SEC)

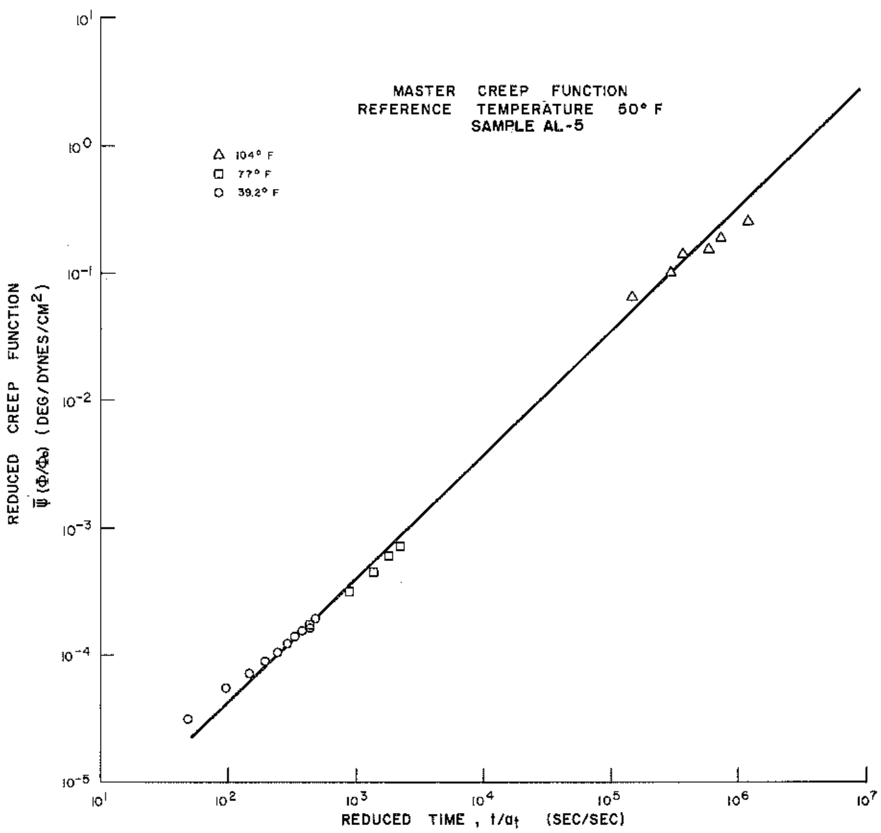
MASTER CREEP FUNCTION
REFERENCE TEMPERATURE 50° F
SAMPLE AL-5
104° F
77° F
39.2° F
REDUCED CREEP FUNCTION
$\bar{\psi}$ (Φ/Φ_0) (DEG/DYNES/CM²)
REDUCED TIME, t/a_T (SEC/SEC)

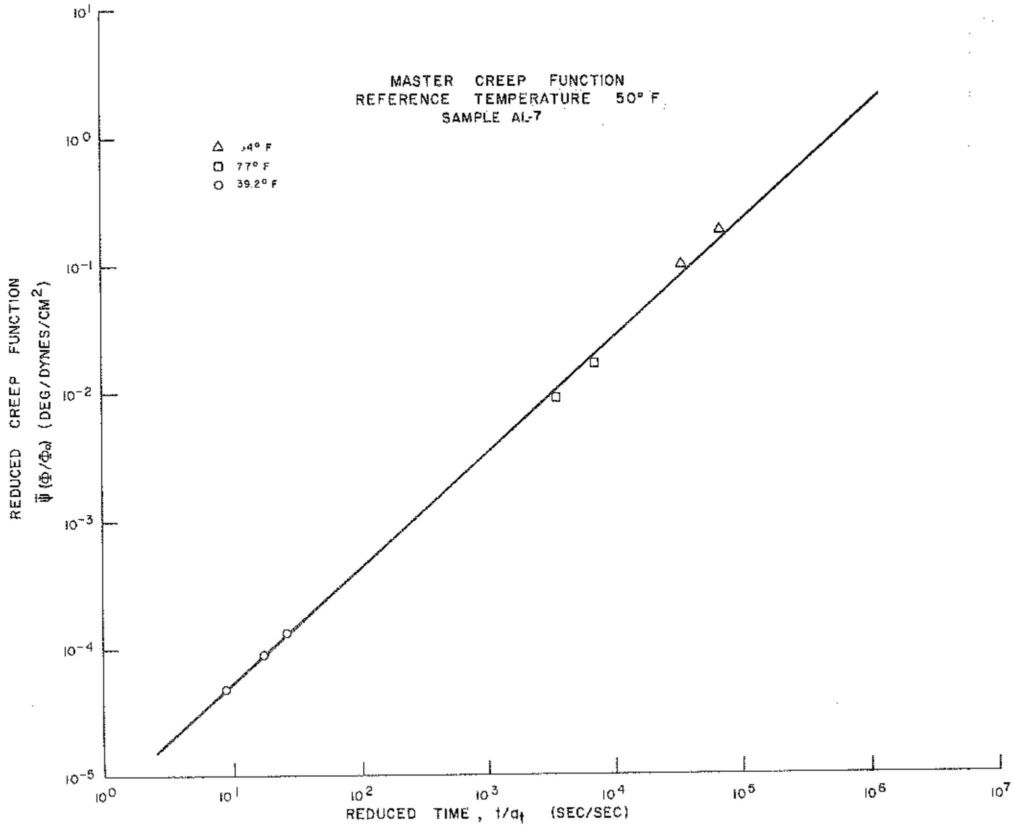
MASTER CREEP FUNCTION
REFERENCE TEMPERATURE 50° F
SAMPLE AL-7
4° F
77° F
39.2° F
REDUCED CREEP FUNCTION
$\bar{\psi}(\Phi/\Phi_0)$ (DEG/DYNES/CM^2)
REDUCED TIME, t/a_t (SEC/SEC)
10^1
10^0
10^{-1}
10^{-2}
10^{-3}
10^{-4}
10^{-5}
10^0 10^1 10^2 10^3 10^4 10^5 10^6 10^7

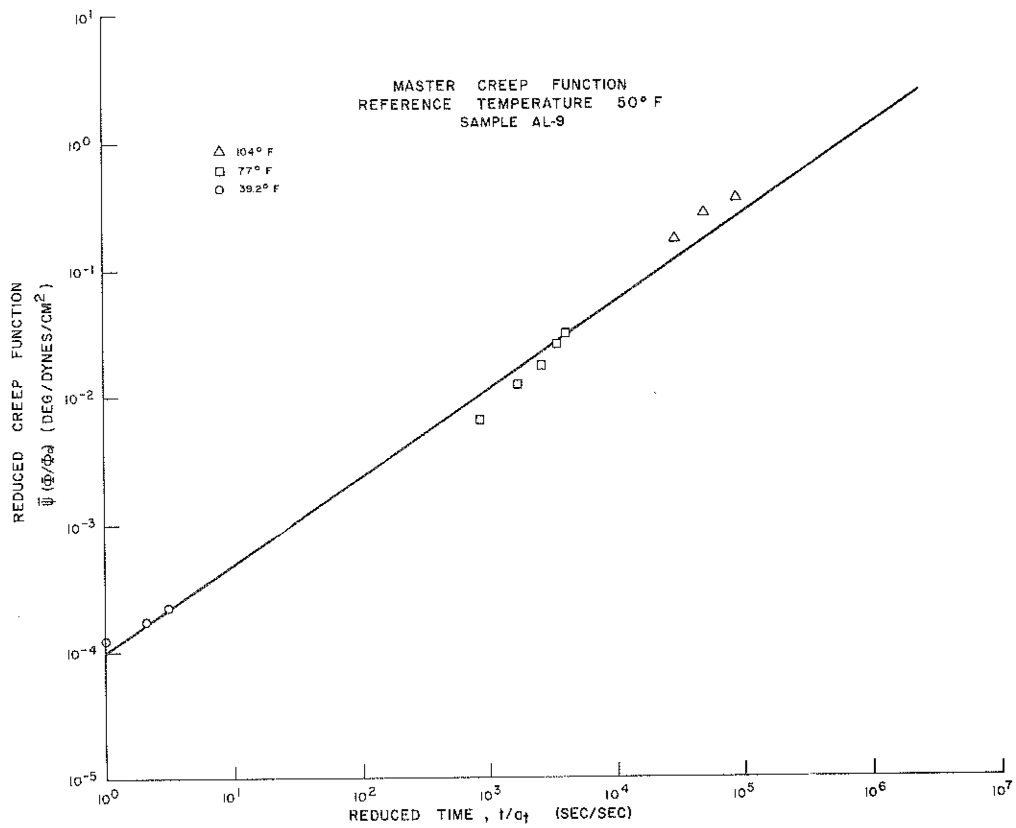
MASTER CREEP FUNCTION
REFERENCE TEMPERATURE 50° F
SAMPLE AL-9
104° F
77° F
39.2° F
REDUCED CREEP FUNCTION
$\bar{\psi}(\Phi/\Phi_0)$ (DEG/DYNES/CM^2)
REDUCED TIME, t/a_t (SEC/SEC)
10^1
10^0
10^{-1}
10^{-2}
10^{-3}
10^{-4}
10^{-5}
10^0 10^1 10^2 10^3 10^4 10^5 10^6 10^7

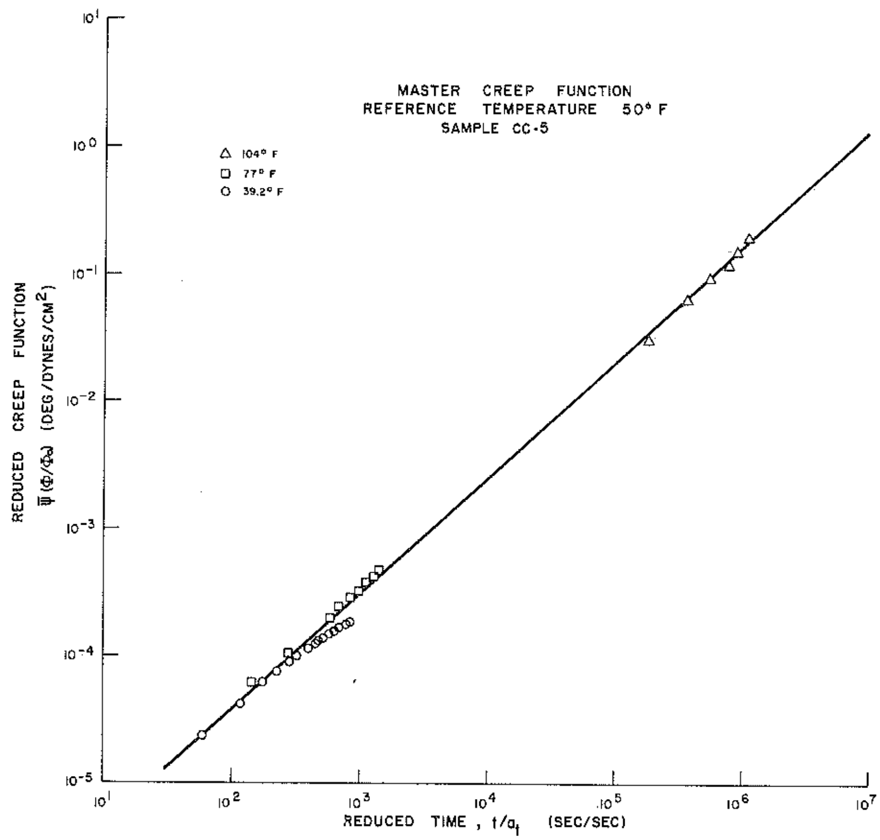
MASTER CREEP FUNCTION
REFERENCE TEMPERATURE 50° F
SAMPLE CC-5
△ 104° F
□ 77° F
○ 39.2° F
REDUCED CREEP FUNCTION
$\bar{\psi}(\Phi/\Phi_0)$ (DEG/DYNES/CM^2)
REDUCED TIME, t/a_t (SEC/SEC)
10^1
10^0
10^{-1}
10^{-2}
10^{-3}
10^{-4}
10^{-5}
10^1
10^2
10^3
10^4
10^5
10^6
10^7

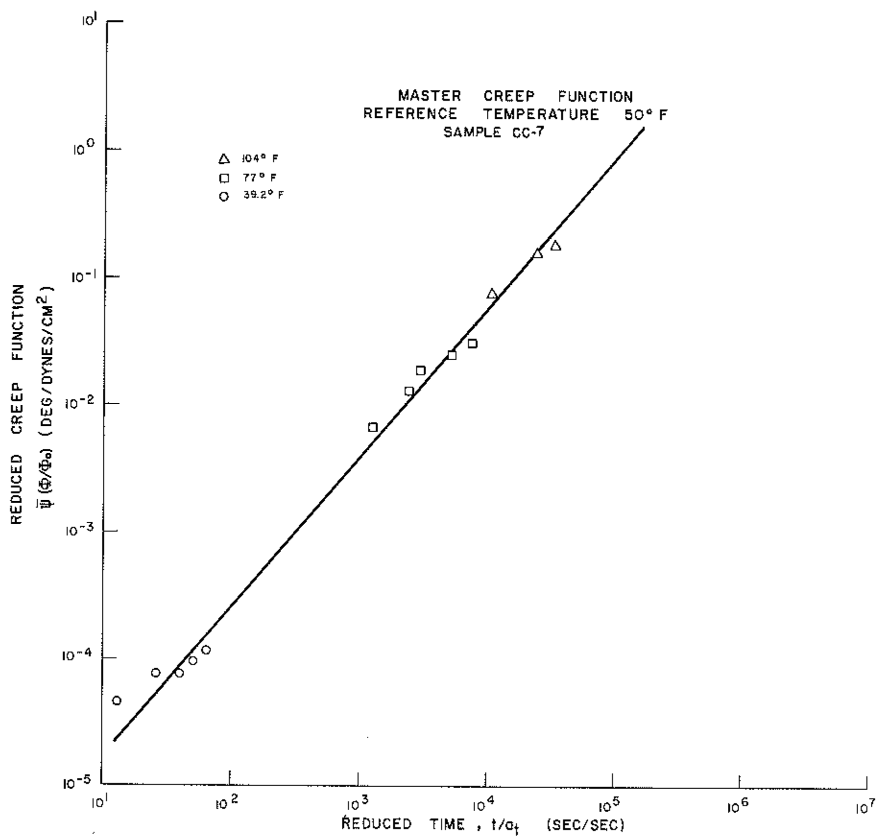
MASTER CREEP FUNCTION
REFERENCE TEMPERATURE 50° F
SAMPLE CC-7
△ 104° F
□ 77° F
○ 39.2° F
REDUCED CREEP FUNCTION
$\bar{\psi}(\Phi/\Phi_0)$ (DEG/DYNES/CM^2)
REDUCED TIME, t/a_t (SEC/SEC)
10^1
10^0
10^{-1}
10^{-2}
10^{-3}
10^{-4}
10^{-5}
10^1
10^2
10^3
10^4
10^5
10^6
10^7

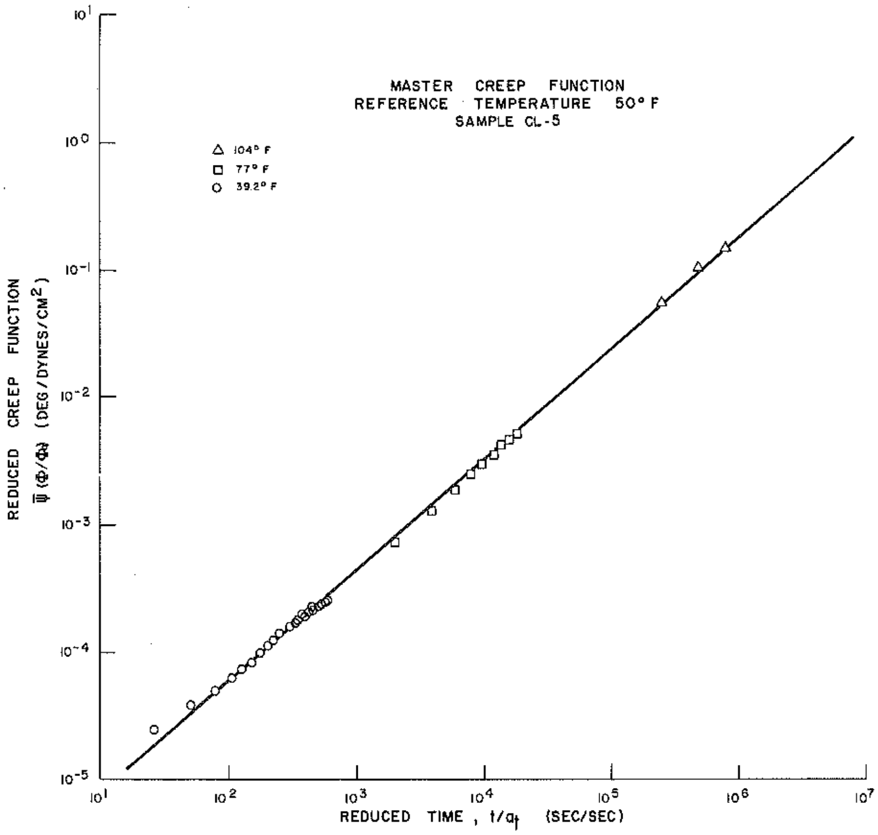
MASTER CREEP FUNCTION
REFERENCE TEMPERATURE 50° F
SAMPLE CL-5
△ 104° F
□ 77° F
○ 39.2° F
REDUCED CREEP FUNCTION
$\bar{\psi}(\Phi/\Phi_0)$ (DEG/DYNES/CM^2)
REDUCED TIME, t/a_t (SEC/SEC)

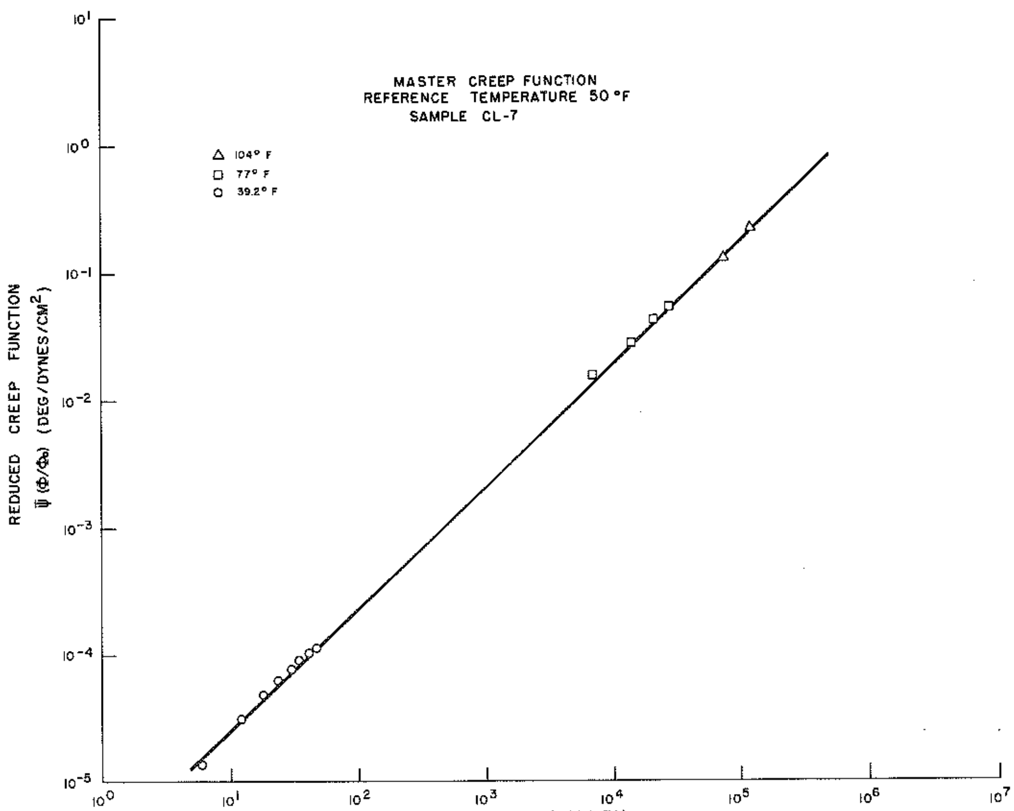
MASTER CREEP FUNCTION
REFERENCE TEMPERATURE 50 °F
SAMPLE CL-7
△ 104° F
□ 77° F
○ 39.2° F
REDUCED CREEP FUNCTION
$\bar{\psi}(\Phi/\Phi_0)$ (DEG/DYNES/CM^2)
REDUCED TIME, t/a_t (SEC/SEC)

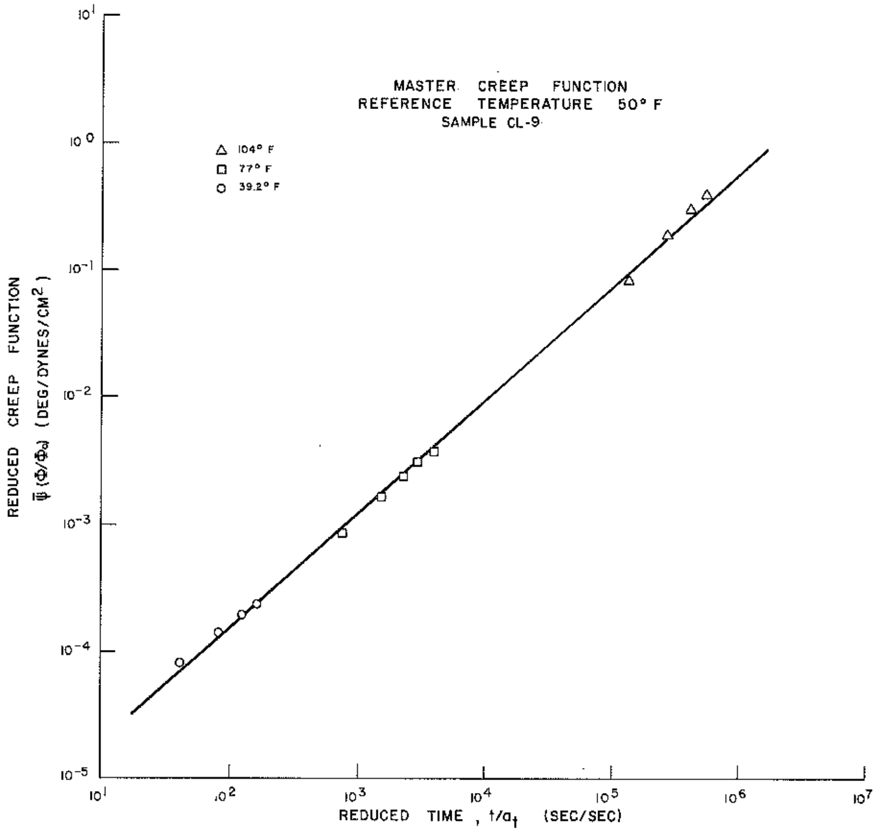
MASTER CREEP FUNCTION
REFERENCE TEMPERATURE 50° F
SAMPLE CL-9
△ 104° F
□ 77° F
○ 39.2° F
REDUCED CREEP FUNCTION
$\bar{\psi}(\Phi/\Phi_0)$ (DEG/DYNES/CM^2)
REDUCED TIME, t/a_t (SEC/SEC)

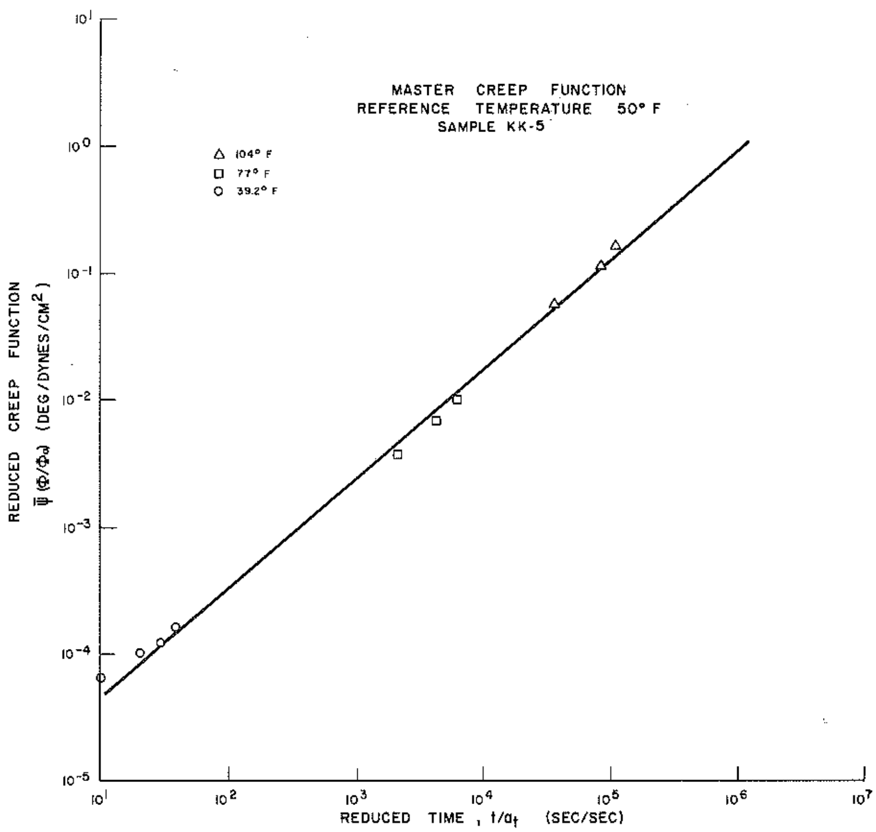
MASTER CREEP FUNCTION
REFERENCE TEMPERATURE 50° F
SAMPLE KK-5
△ 104° F
□ 77° F
○ 39.2° F
REDUCED CREEP FUNCTION
$\bar{\psi}(\Phi/\Phi_0)$ (DEG/DYNES/CM^2)
REDUCED TIME, t/a_t (SEC/SEC)

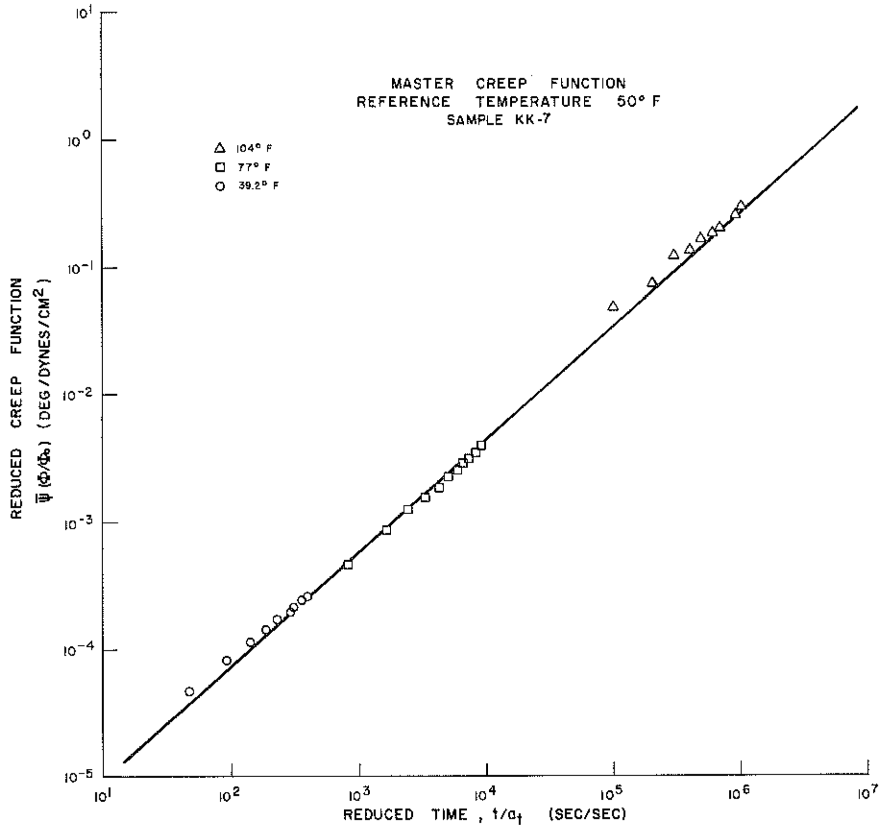
MASTER CREEP FUNCTION
REFERENCE TEMPERATURE 50° F
SAMPLE KK-7
△ 104° F
□ 77° F
○ 39.2° F
REDUCED CREEP FUNCTION
$\bar{\psi}(\Phi/\Phi_0)$ (DEG/DYNES/CM^2)
REDUCED TIME, t/a_t (SEC/SEC)

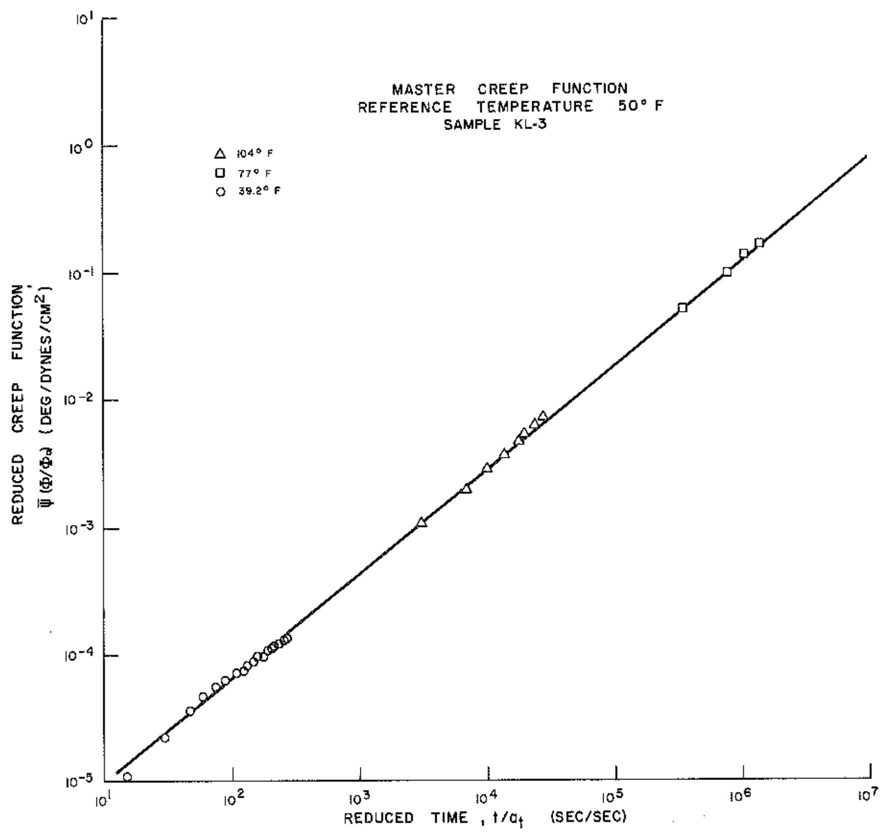
MASTER CREEP FUNCTION
REFERENCE TEMPERATURE 50° F
SAMPLE KL-3
△ 104° F
□ 77° F
○ 39.2° F
REDUCED CREEP FUNCTION
$\bar{\psi}(\Phi/\Phi_0)$ (DEG/DYNES/CM^2)
REDUCED TIME, t/a_t (SEC/SEC)

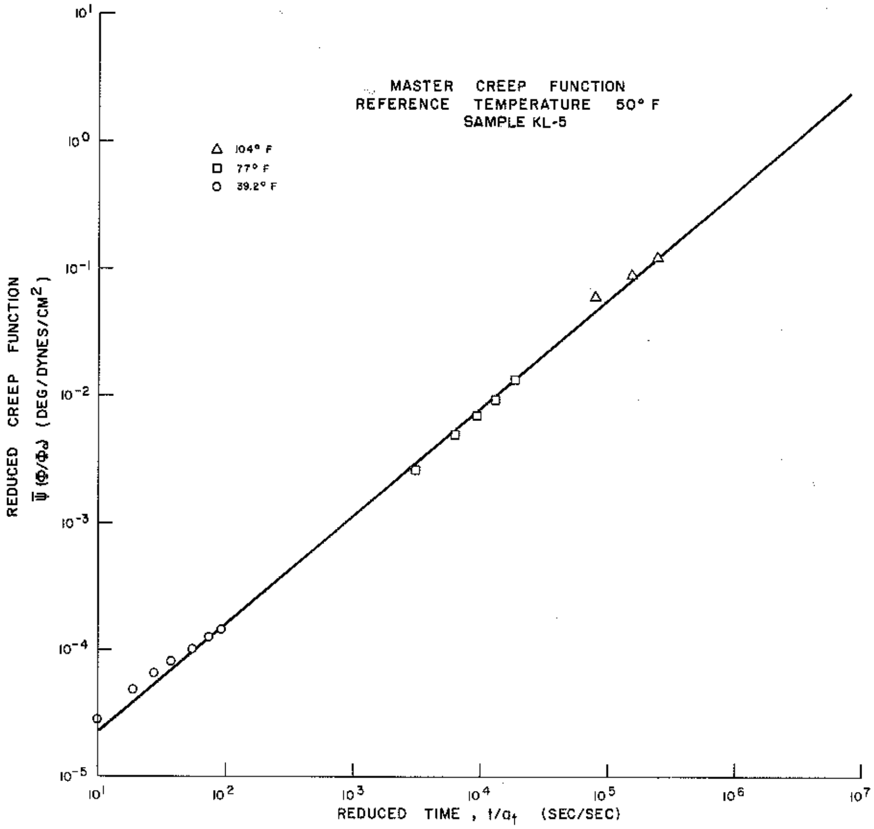
MASTER CREEP FUNCTION
REFERENCE TEMPERATURE 50° F
SAMPLE KL-5
104° F
77° F
39.2° F
REDUCED CREEP FUNCTION
$\bar{\psi}$ (Φ/Φ_o) (DEG/DYNES/CM^2)
REDUCED TIME , t/a_t (SEC/SEC)

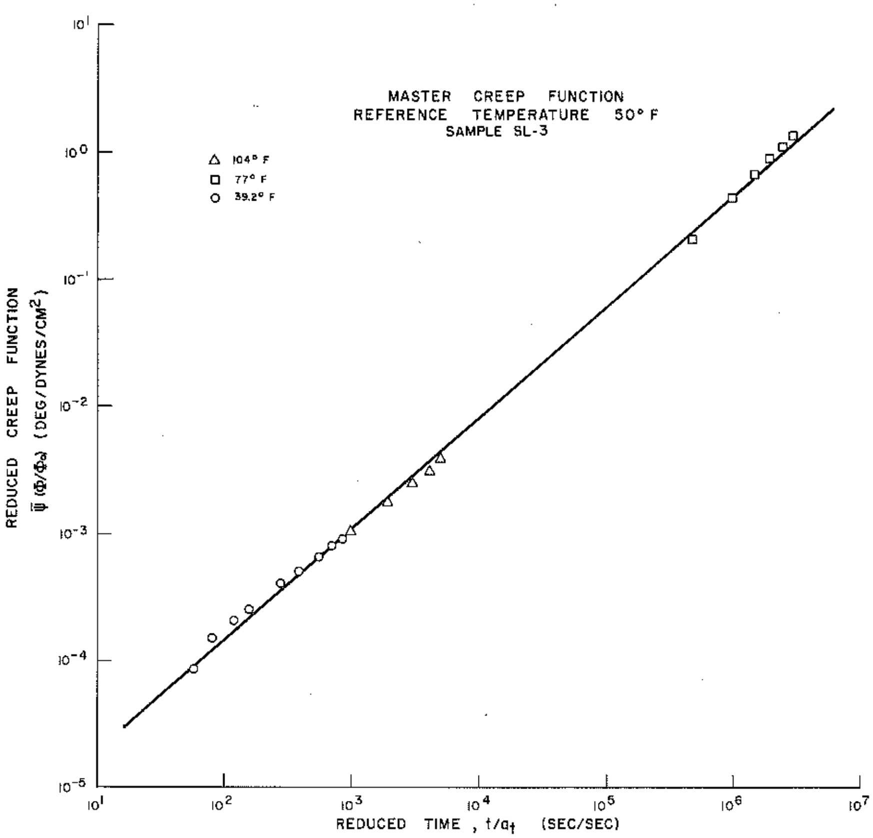
MASTER CREEP FUNCTION
REFERENCE TEMPERATURE 50° F
SAMPLE SL-3
104° F
77° F
39.2° F
REDUCED CREEP FUNCTION
$\bar{\psi}$ (Φ/Φ_o) (DEG/DYNES/CM^2)
REDUCED TIME , t/a_t (SEC/SEC)

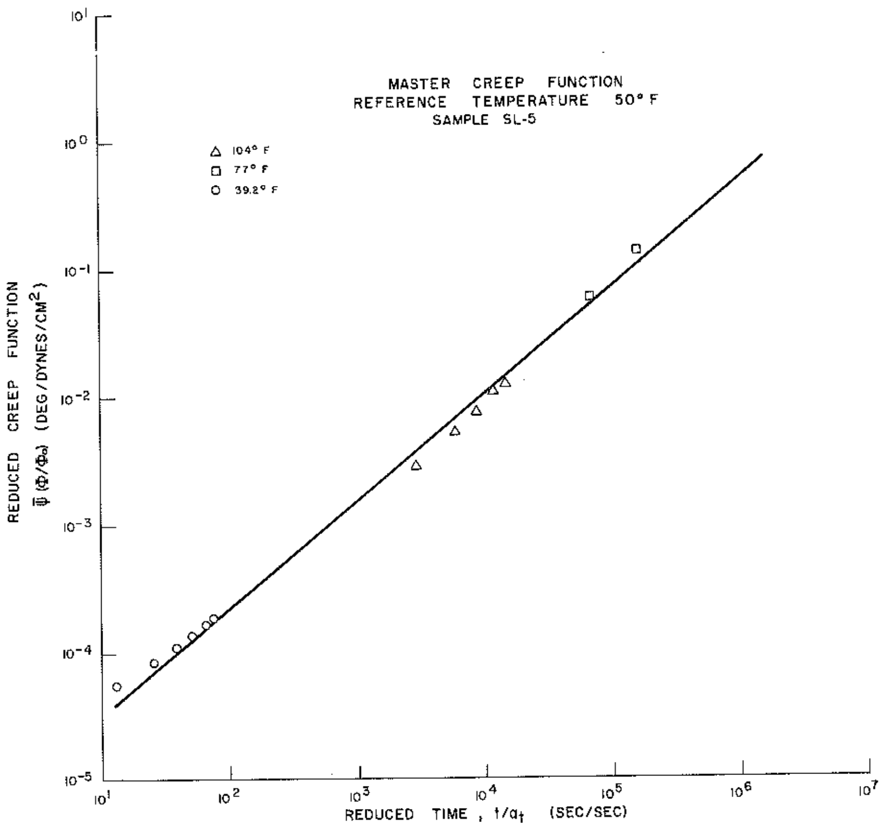

MASTER CREEP FUNCTION
REFERENCE TEMPERATURE 50° F
SAMPLE SL-5
△ 104° F
□ 77° F
○ 39.2° F
REDUCED CREEP FUNCTION
$\Psi(\Phi/\Phi_o)$ (DEG/DYNES/CM^2)
REDUCED TIME, t/a_t (SEC/SEC)
10^1
10^0
10^{-1}
10^{-2}
10^{-3}
10^{-4}
10^{-5}
10^1
10^2
10^3
10^4
10^5
10^6
10^7